S-wave optical potential in pionic atoms

C. García-Recio
Departamento de Física Teórica, Facultad de Ciencias, Valladolid, Spain
and Center for Theoretical Physics, Laboratory for Nuclear Science, and Department of Physics, Massachusetts Institute of Technology, Cambridge, Massachusetts 02139

E. Oset
Departamento de Física Teórica, Facultad de Ciencias Físicas, Universidad de Valencia, Burjasot (Valencia), Spain

L. L. Salcedo*
Center for Theoretical Physics, Laboratory for Nuclear Science, and Department of Physics, Massachusetts Institute of Technology, Cambridge, Massachusetts 02139
(Received 19 March 1987)

We present a new formal approach for the calculation of the s-wave optical potential for pionic atoms which makes extensive use of the Lindhard function, its analytical properties, and its useful low density limit. The conventional parameters b_0 and B_0 are calculated and compared to results from empirical fits to pionic atom data. We show that the virtual excitation of ph-Δh components by the pion is the main source of the real part of B_0. Higher order effects from the polarization of the pion lead to some enhancement of $\mathrm{Im}B_0$, providing values which are compatible with the empirical data. The real part of the potential suffers from larger uncertainties due to the off-shell extrapolation of the πN scattering amplitude.

I. INTRODUCTION

The properties of pionic atoms have been traditionally studied in terms of a pion-nucleus optical potential that contains an s-wave part and a p-wave part.[1] The s-wave part, which is the subject of this paper, is given by

$$2\omega V_{\mathrm{opt}}(r)=-4\pi\left[(1+\epsilon)b_0\rho(r)+(1+\epsilon)b_1[\rho_n(r)-\rho_p(r)]+\left[1+\frac{\epsilon}{2}\right]B_0\rho^2(r)\right], \tag{1.1}$$

with ρ_p,ρ_n the proton and neutron densities and $\rho=\rho_n+\rho_p$, ω the pion energy, and $\epsilon=\mu/m$ the ratio of the pion to the nucleon mass. The following relationship[1] between b_0, b_1, and the isospin $\frac{1}{2},\frac{3}{2}$ scattering lengths a_1,a_3 holds:

$$b_0=\tfrac{1}{3}(a_1+2a_3)\ ,\qquad b_1=-\tfrac{1}{3}(a_1-a_3)\ . \tag{1.2}$$

Values for a_1,a_3 can be found in Ref. 2:

$$a_1=(0.171\pm0.004)\mu^{-1}\ ,\qquad a_3=(-0.105\pm0.003)\mu^{-1}\ . \tag{1.3}$$

Because of a large cancellation in (1.2), b_0 has an abnormally small value, $b_0=-0.013\mu^{-1}$, compared to $b_1=-0.092\mu^{-1}$. Because of this cancellation, small corrections tend to influence the s-wave part of the potential appreciably. One correction which is customarily included in the first order optical potential (ρ term) is the Pauli corrected s-wave rescattering piece.[1,3]

With the potential of Eq. (1.1), together with the p-wave part, one can carry out fits to the shifts and widths of the pionic atom levels. By fixing the parameter b_0, this fit provides empirical values for the complex second order parameter B_0. The parameter B_0 has an imaginary part which is meant to account for pion absorption, a process that in free space cannot occur in a single nucleon and is extraordinarily suppressed in finite nuclei, although the conservation of energy and momentum allows for it to occur in bound nucleons. The most simple assumption is that pion absorption takes place through pairs of nucleons and this justifies the empirical form for this part of the optical potential as a $\rho^2(r)$ functional.[1] The assumption of absorption by a pair of nucleons has received strong theoretical support from a recent work which explicitly calculates the contribution from two-body to three-body absorption in the p wave.[4,5] The results there show that more than 95% of the absorption at threshold takes place through pairs of nucleons. The arguments used there can be easily extrapolated to the s-wave part, and one should expect similar results for this case. This does not mean that the form of the potential should be of the ρ^2 type. Integration over the Fermi sea momenta, the effect of the Pauli exclusion principle, and other many-body effects actually produce diversions from the ρ^2 functional.

The ρ^2 functional for the second order optical potential is, however, a natural and useful way of parametrizing this part of the optical potential, and its tremedous success[1,6–14] in correlating a large amount of experimental data[15–17] deserves obvious recognition. A recent study of the correlations between the second order and first order parts of the optical potential shows, however,

that the shape of the potential is not too important since one can get equally good fits by changing simultaneously the b_0 and B_0 parameters in an appropriate way.[14] This suggests the existence of an effective density which the pions "feel" when they interact strongly with the nucleus.[14] This can explain why such good fits to the data can be obtained with the potential (1.1) or with other theoretical based functionals of ρ which differ appreciably from the ρ or ρ^2 form.[18]

We now show a couple of best fit parameters:

b_0	B_0
$-0.017\mu^{-1}$	$(-0.049+i0.046)\mu^{-4}$ (Ref. 7)
$-0.030\mu^{-1}$	$(0.000+i0.050)\mu^{-4}$ (Ref. 11)

(1.4)

These results show that $\mathrm{Im}B_0$ is rather constant in different approaches, while b_0, and $\mathrm{Re}B_0$ are not so well determined.

With respect to the theoretical approach to this part of the optical potential, there has been a substantial amount of work done.[19–30] The most common approach in order to consider the s-wave pion absorption by pairs of particles is shown diagrammatically in Fig. 1. A pion collides with one nucleon through the s-wave part of the πN t matrix (solid circle in the figure). The scattered pion now travels virtually through the nucleus carrying part of the energy and momentum to a second nucleon.

The part of the optical potential that contains the absorption mechanism of Fig. 1 is given in Fig. 2 in the form of a many-body Feynman diagram. The πNN vertex in Fig. 1, where the scattered pion is absorbed, is the standard πNN Yukawa p-wave coupling.

The imaginary part from the diagram in Fig. 2 for pions at threshold will come from the analytical cut corresponding to the horizontal line in the figure; in other words, from the situation where the particles cut by the horizontal line are placed onshell. This is obviously the pion absorption process, with the pion exciting two particles and two holes or, equivalently, pion absorption through the process of Fig. 1.

The mechanism of Fig. 1 has been checked in pion absorption by deuterons or in the related $\mathrm{NN}\rightarrow\pi\mathrm{d}$ reaction with good results.[31,32] It has also been successfully used in the study of proton induced pion production in nuclei, i.e., inclusive (p,π) reactions, close to threshold.[33]

In addition to the imaginary part of the diagram in Fig. 2, which we have discussed, there is also a real part

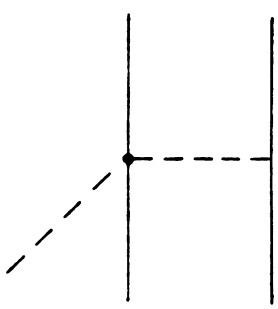

FIG. 1. Diagrammatic representation of s-wave pion absorption. The solid circle stands for the πN s-wave t matrix.

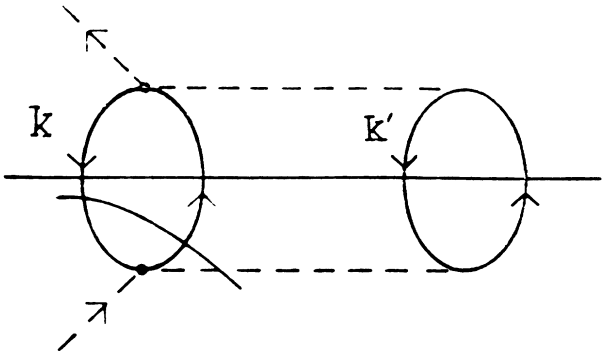

FIG. 2. Many-body diagram of the pion nucleus optical potential that contains the absorption mechanism of Fig. 1. The straight horizontal line indicates the absorption cut. It gives rise to an imaginary part of the optical potential when the two-particle— two-hole states are placed on shell. The curved line indicates the quasielastic cut and gives rise to an imaginary part when a ph and a pion are placed on shell.

associated with it, necessarily linked to this imaginary part because of the analytical properties of the optical potential. One can directly evaluate the real and imaginary parts of the diagram or evaluate the imaginary part and later use dispersion relations in order to evaluate the real part, which is often used in the literature.

If one wishes to summarize the theoretical results, one could say that, on the average, the results for $\mathrm{Im}B_0$ are from $\frac{1}{2}$ to $\frac{2}{3}$ of the empirical results and $\mathrm{Re}B_0$ is of the order of magnitude of $\mathrm{Im}B_0$ and of positive sign. Hence the results for $\mathrm{Im}B_0$ are systematically too small, while the results for $\mathrm{Re}B_0$ have an opposite sign to those that one gets from bets fits, Eq. (1.4). As an example, we quote two different results. Reference 28 has $\mathrm{Im}B_0=0.036\mu^{-4}$ and $\mathrm{Re}B_0=2.6\,\mathrm{Im}B_0$. Reference 29 gives $\mathrm{Im}B_0\approx(0.020-0.027)\mu^{-4}$ and $\mathrm{Re}B_0\approx0.008\mu^{-4}$, although the authors offer this last magnitude as a lowest one.

The agreement of the different authors on the sign of $\mathrm{Re}B_0$ is remarkable, with some exceptions, such as the one in the early work of Ref. 22, done under assumptions which turn out to be incorrect when more accurate calculations are carried out.[28]

In view of these persistent discrepancies between theoretical and empirical values of the s-wave optical potential parameters, a thorough revision of the problem—by looking at all the approximations done in former calculations and trying to improve all of them systematically—has seemed advisable to us. At the same time we have also introduced new pieces which affect the real part and which had been neglected before.

The usual approximations where the improvements have been done are the following:

(1) In the calculation of $\mathrm{Im}B_0$ from the diagram in Fig. 2, the effects of the Pauli blocking in the particle states are generally neglected. They are taken into account in the 2p-2h excitation of Ref. 30, though with a model quite different to the one we study here.

(2) As we have mentioned, most of the approaches use a dispersion relation to calculate $\mathrm{Re}B_0$ once $\mathrm{Im}B_0$ is cal-

culated as a function of the energy. However, as we have pointed out before, at threshold the only source of the imaginary part in the diagram of Fig. 2 corresponds to the absorption cut, where the pion energy goes into exciting two particles and two holes. However, when we increase the pion energy, a new channel, the quasielastic, is open, and one also gets the imaginary part from this source. A dispersion relation requires the use of $\mathrm{Im}B_0$ for different energies. Hence the source of $\mathrm{Im}B_0$ will come from both the absorption and the quasielastic cuts. Thus the real part of B_0 will be influenced by both sources of $\mathrm{Im}B_0$. The different approaches so far have paid attention to the absorption cut and neglected the second. Our formalism, which pays particular attention to the analytical structure of the diagrams, finds a consistent and satisfactory answer to this problem by directly calculating the real part of the diagram at threshold, without the need of a dispersion relation and the evaluation of the quasielastic cut.

(3) A look at the diagram in Fig. 2 shows that the intermediate pions are off shell. Hence one needs the πN s-wave amplitude off shell in order to evaluate B_0. The same can be said about the off-shell effects affecting the lowest order part of the optical potential. In nuclear matter the pions necessarily scatter in the forward direction; there is conservation of four-momentum. Hence the optical potential will require the πN amplitudes on shell, as one assumes implicitly in Eq. (1.1). However, in a finite nucleus, where the single particle states are eigenstates of the energy but not of momentum, only the pion energy is conserved in the collision, not the momentum. Situations where the pions are off shell can then occur in intermediate steps which lead from the optical potential to the π-nucleus T matrix. This automatically leads to modifications in the lowest order part of the optical potential.[34,35]

(4) If one cuts the two intermediate pions in Fig. 2 by a vertical line and looks at the diagram remaining on the right-hand side, it looks like the renormalization of a pion in nuclear matter through ph excitation. The $\Delta(\frac{3}{2},\frac{3}{2})$ degrees of freedom in such processes have been repeatedly emphasized[36,37] and they play an important role in the dressing up of pions inside matter. Thus in addition to the ph excitation of the pion, we will also consider Δh excitation, as shown in Fig. 3. This will not contribute to the imaginary part of B_0, but it will contribute to the real part, and actually quite strongly as we shall see. This reflects once more the difficulties encountered in evaluating $\mathrm{Re}B_0$ through a dispersion relation. The fact that the diagram of Fig. 3 gives an important contribution to $\mathrm{Re}B_0$ implies that in a dispersion relation approach one should have evaluated $\mathrm{Im}B_0$ at energies sufficiently high that the channel $\pi\mathrm{NN}\rightarrow\pi\mathrm{N}\Delta$ would be physically open.

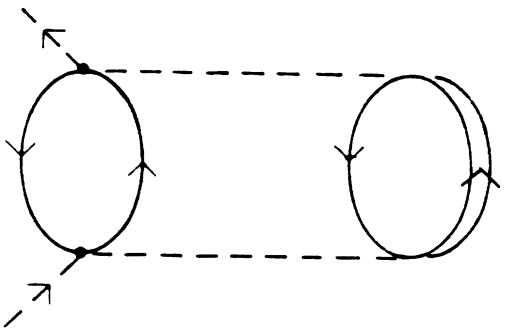

FIG. 3. Many-body diagram for the pion self-energy (or equivalently pion-nucleus optical potential), through ph-Δh excitation, which gives rise to a real part of the self-energy at threshold.

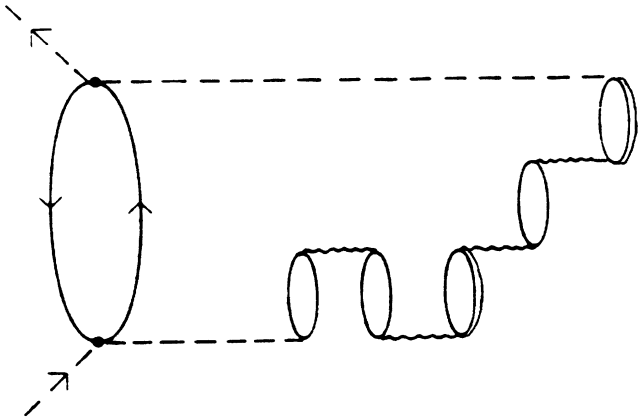

FIG. 4. Higher order terms of the diagrams of Figs. 2 and 3 which come from the polarization of the pion.

(5) By following the line introduced in the former point, we would like to dress up the pion propagator not only by a single ph or Δh excitation, but we would like to have the full series of reducible diagrams that gives rise to the pion propagator in the medium.[36] This leads to the iteration of the ph or Δh excitation in the way shown in Fig. 4. In the wavy lines, however, other ingredients of the ph interaction, in addition to one-pion exchange, will be included.[37]

(6) In addition to the diagram of Fig. 4, crossed terms and exchange terms corresponding to this diagram are equally calculated.

The paper continues, with Sec. II devoted to the formalism of the s-wave absorption; Sec. III deals with the exchange and Δ terms; Sec. IV is devoted to the study of the effects of the Pauli exclusion principle; Sec. V deals with off-shell effects and short-range correlations; in Sec. VI we introduce higher order contributions in the density expansion. Section VII deals with the influence of the off-shell extrapolation on the lowest order parameter b_0 and in Sec. VIII we summarize our conclusions.

II. FORMALISM FOR S-WAVE ABSORPTION

We will start by evaluating the contribution to the optical potential from the diagram in Fig. 2. We need two ingredients, the s-wave part of the πN t matrix and the πNN coupling. For the πNN coupling we will take the usual Yukawa interaction given by

$$\delta H_{\pi\mathrm{NN}}(x)=-ig\bar{\psi}(x)\gamma_5\tau^\lambda\phi^\lambda(x)\psi(x)\ , \tag{2.1}$$

where $\psi(x)$ is the nucleon field and $\phi^\lambda(x)$ is the pion field

of isospin λ. On the other hand, in order to account for the πN s-wave amplitude, we will use a popular phenomenological interaction Lagrangian given by[38]

$$\delta H_{\pi N}^{(s)}(x)=4\pi\left[\frac{\lambda_1}{\mu}\bar{\psi}(x)\boldsymbol{\phi}(x)\cdot\boldsymbol{\phi}(x)\psi(x)+\frac{\lambda_2}{\mu^2}\bar{\psi}(x)\tau\cdot[\boldsymbol{\phi}(x)\times\partial_t\boldsymbol{\phi}(x)]\psi(x)\right], \quad (2.2)$$

where λ_1,λ_2 are related to the isoscalar b_0 and isovectorial b_1 scattering lengths by means of the relationships

$$(1+\epsilon)b_0=-\frac{2\lambda_1}{\mu}, \qquad (1+\epsilon)b_1=-\frac{2\lambda_2}{\mu}. \quad (2.3)$$

In order to evaluate the optical potential (1.1) corresponding to the diagram of Fig. 2 we will use the standard Feynman rules in momentum space.[39] The vertices corresponding to Eqs. (2.1) and (2.2), which are shown diagrammatically in Fig. 5, are given by

$$\delta\tilde{H}_{\pi NN}=i\frac{f}{\mu}\langle m_s'\mid\boldsymbol{\sigma}\cdot\mathbf{q}\mid m_s\rangle\langle m_t'\mid\tau^\lambda\mid m_t\rangle, \quad (2.4a)$$

$$\delta\tilde{H}_{\pi N}^{(s)}=4\pi\delta_{m_s m_s'}\left[\frac{2\lambda_1}{\mu}\delta_{m_t' m_t}\delta_{\lambda'\lambda}-i\epsilon_{\alpha\lambda'\lambda}\frac{\lambda_2}{\mu^2}(q^0+q^{0\prime})\langle m_t'\mid\tau^\alpha\mid m_t\rangle\right], \quad (2.4b)$$

where $f/\mu=g/2m$, and we have used the nonrelativistic reduction for the γ_5 coupling of Eq. (2.1).

With these ingredients it is now easy to calculate the contribution of the diagram of Fig. 2. For the pion self-energy Π, related to the optical potential as $V_{\rm opt}=\Pi(p)/2p^0$, one obtains

$$\Pi(p)=i\int\frac{d^4q}{(2\pi)^4}U_N(p-q)D_0^2(q)\frac{f^2(q^2)}{\mu^2}U_N(q)\mathbf{q}^2\times(4\pi)^2\left[\left[\frac{2\lambda_1}{\mu}\right]^2+2\left[\frac{\lambda_2}{\mu^2}(p^0+q^0)\right]^2\right], \quad (2.5)$$

where p,q are the momenta of external and intermediate pions, respectively. In Eq. (2.5), $D_0(q)$ is the free pion propagator,

$$D_0(q)=\frac{1}{q^{02}-\mathbf{q}^2-\mu^2+i\eta}, \quad (2.6)$$

and $U_N(q)$ is the useful Lindhard function,[40] defined as

$$U_N(q)=-4i\int\frac{d^4k}{(2\pi)^4}G_0(k)G_0(k+q), \quad (2.7)$$

with G_0 the Pauli corrected nucleon propagator

$$G_0(k)=\frac{1-n(\mathbf{k})}{k^0-\varepsilon(\mathbf{k})+i\eta}+\frac{n(\mathbf{k})}{k^0-\varepsilon(\mathbf{k})-i\eta}=\frac{1}{k^0-\varepsilon(\mathbf{k})+i\eta}+2\pi i n(\mathbf{k})\delta(k^0-\varepsilon(\mathbf{k}))\equiv G_0^{\rm free}(k)+\delta G_P(k), \quad (2.8)$$

with $n(\mathbf{k})$ the occupation number and $\varepsilon(\mathbf{k})$ the kinetic energy of the nucleon. Equation (2.8) explicitly shows the Pauli correction to the free nucleon propagator. By carrying out the k^0 integration in (2.7), $U_N(q)$ can be rewritten as

$$U_N(q)=4\int\frac{d\mathbf{k}}{(2\pi)^3}\left[\frac{n(\mathbf{k})[1-n(\mathbf{k}+\mathbf{q})]}{q^0-\varepsilon(\mathbf{k}+\mathbf{q})+\varepsilon(\mathbf{k})+i\eta}+\frac{n(\mathbf{k}+\mathbf{q})[1-n(\mathbf{k})]}{-q^0-\varepsilon(\mathbf{k})+\varepsilon(\mathbf{k}+\mathbf{q})+i\eta}\right], \quad (2.9)$$

where a factor 4 is introduced for convenience to account for the spin and isospin degrees of freedom. Explicit expressions for the real and imaginary parts of $U_N(q)$ can be found in Ref. 40 for real values of q^0, and in Refs. 39 and 41 for complex values of q^0, which are needed in the present work.

The first thing to note is that Eq. (2.9) contains both the direct and the crossed ph excitation terms which means that by using the Lindhard functions in (2.5) we will automatically account for all the diagrams in Fig. 6. The last three diagrams will not contribute to the imaginary part of the optical potential, but will give some

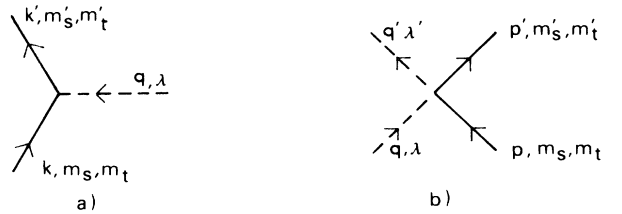

FIG. 5. Vertices for the πNN interaction and the s-wave πN scattering matrix.

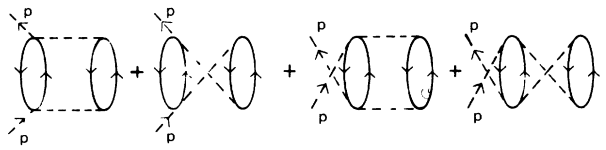

FIG. 6. Set of diagrams for the pion self-energy taken into account automatically by means of the Lindhard function U_N in Eqs. (2.5).

contribution to the real part. A fact worth mentioning is the analytical structure of the Lindhard function, with the function $U_N(q)$ continuous for complex values of q^0 in the first and third quadrants.

In (2.5) we have introduced the q dependence of the p-wave πNN coupling to account for off-shell effects. We will deal with the s-wave off-shell extrapolation later on. The p-wave πNN coupling has been studied thoroughly through analysis of many different processes where the pions are off shell. Studies from π absorption in the deuteron,[31,32] np and $\bar{p}p$ charge exchange scattering,[42] dispersion theoretical analysis,[43] quasi-two-body hadronic reactions,[44] or the NN interaction[45] indicate that the off-shell dependence of the vertex can be parametrized by means of a monopole form factor. Thus we have

$$\frac{f(q^2)}{\mu}=\frac{f}{\mu}\left[\frac{\Lambda^2-\mu^2}{\Lambda^2-q^2}\right], \tag{2.10}$$

with q the pion four-momentum and $\Lambda\simeq 1000-1500$ MeV.

The q^0 integration in problems similar to the one here is normally carried out by closing some contour over the complex plane q^0. However, such a procedure is impracticable here because $U_N(q)$ and $U_N(p-q)$ have cuts on opposite sides of the real axis.

In order to be able to exploit the analytical properties of (2.5) to carry out the q^0 integration, we will make use of a Lehmann representation which allows us to express the Lindhard function in terms of its imaginary part for real values of the energy variable:

$$U(q^0,q)=\int_0^\infty \frac{d\omega'}{\pi}\frac{-2\omega'\,\mathrm{Im}U(\omega',q)}{q^{02}-\omega'^2+i\eta}\,. \tag{2.11}$$

By using (2.11) to express $U_N(p-q)$, Eq. (2.5) can now be rewritten as

$$\Pi(p)=i\int_{-\infty}^{+\infty}\frac{dq^0}{(2\pi)}\int\frac{d\mathbf{q}}{(2\pi)^3}\int_0^\infty\frac{d\omega'}{\pi}\frac{-2\omega'\mathrm{Im}U_N(\omega',\mathbf{p}-\mathbf{q})}{(p^0-q^0)^2-\omega'^2+i\eta}$$

$$\times(4\pi)^2D_0^2(q)\frac{f^2(q^2)}{\mu^2}U_N(q)\mathbf{q}^2\left[\left[\frac{2\lambda_1}{\mu}\right]^2+2\left[\frac{\lambda_2}{\mu^2}(p^0+q^0)\right]^2\right]. \tag{2.12}$$

The analytical structure of the integrand for q^0 is now simplified since we have replaced the cut of $U_N(p-q)$ by the integral over ω' of single poles. This analytical structure is shown in Fig. 7 and immediately suggests that we do a Wick rotation in order to avoid the cuts of $U_N(q)$. Note that the poles of $D_0(q)$ are in the same situation as the cuts of $U_N(q)$. By carrying the q^0 integration over the contour shown in Fig. 7, we obtain

$$\Pi(p)=i\int_{-i\infty}^{+i\infty}\frac{dq^0}{2\pi}\int\frac{d\mathbf{q}}{(2\pi)^3}U_N(p^0-q^0,\mathbf{p}-\mathbf{q})F(p,q)-\int\frac{d\mathbf{q}}{(2\pi)^3}\int_0^{p_0}\frac{d\omega'}{\pi}\mathrm{Im}U_N(\omega',\mathbf{p}-\mathbf{q})F(p,q)\Big|_{q^0=p_0-\omega'}, \tag{2.13}$$

where

$$F(p,q)=D_0^2(q)\frac{f^2(q^2)}{\mu^2}U_N(q)\mathbf{q}^2(4\pi)^2\left[\left[\frac{2\lambda_1}{\mu}\right]^2+2\left[\frac{\lambda_2}{\mu^2}(p^0+q^0)\right]^2\right]. \tag{2.14}$$

The first term in (2.13) is a real background since there is a cancellation of the imaginary parts of the integral for values of q^0 and $-q^0$ on the imaginary axis. Thus, the imaginary part of $\Pi(p)$ comes only from the second term of (2.13). It can either come from the imaginary part of $U_N(q)$ in $F(p,q)$ (pion absorption into 2p-2h), or through the pole in $D_0(q)$ (quasielastic contribution). At threshold the quasielastic channel is not open and thus the absorption contribution to the imaginary part is the only one that occurs. Thus we have

$$\mathrm{Im}\Pi(p)=-\int\frac{d\mathbf{q}}{(2\pi)^3}\int_0^{p_0}\frac{d\omega'}{\pi}\mathrm{Im}U_N(\omega',\mathbf{p}-\mathbf{q})\frac{f^2(q^2)}{\mu^2}D_0^2(q)$$

$$\times\mathrm{Im}U_N(q)\mathbf{q}^2(4\pi)^2\left[\left[\frac{2\lambda_1}{\mu}\right]^2+2\left[\frac{\lambda_2}{\mu_2}(p^0+q^0)\right]^2\right]\Big|_{q^0=p^0-\omega'}. \tag{2.15}$$

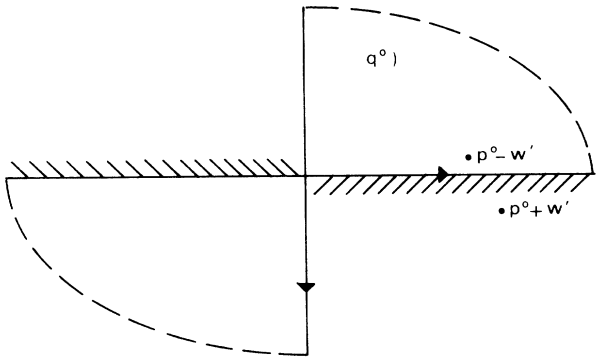

FIG. 7. Analytical structure the Lindhard function $U_N(q)$. The hatching indicates the cuts of $U_N(q)$. In the first and third quadrants $U_N(q)$ is a continuous function in the complex variable q^0. Path followed by the Wick rotation of Eqs. (2.12) and (2.13), with indication of the poles and cuts of the integrand.

This equation has a very clear physical interpretation. The imaginary part of the $U_N(q)$ function appears when a real ph excitation can be done with energy q^0 and momentum $\mathbf{q}$. Thus, in (2.15) the energy of the pion is split into two parts, ω' and q^0, with clear limits for the values of ω', $\omega' \in [0,p^0]$, and $q^0=p^0-\omega'$. With the energy ω' one excites one particle-hole, with the particle and hole on shell, and with the rest of the energy one excites a second ph with the particle and hole on shell. The range of the $\mathbf{q}$ integration is automatically limited, because for fixed energy there is only a limited range of momentum for which $U_N(q)$ has imaginary part.

Equation (2.15) gives the imaginary part of $\Pi(p)$ at threshold coming from pion absorption into 2p-2h. At higher energies we would also get an imaginary part from the pole of $D_0(q)$ in Eq. (2.13). However, the formula in (2.15) can still be used to calculate the contribution to the imaginary part of $\Pi(p)$ from pion absorption.

Before we proceed to make improvements in (2.13)–(2.15) and add extra terms, it is quite illustrating to make some approximations in (2.15) in order to get an easy analytical formula. We will make use of the small density limit where $\mathrm{Im}U_N(q)$ has a trivial representation:

$$i\,\mathrm{Im}U_N(q) \underset{\rho\to 0}{\to} 4\int \frac{d\mathbf{k}}{(2\pi)^3} n(\mathbf{k})(-i)\pi\delta\left[|q^0| - \frac{\mathbf{q}^2}{2m}\right] = -i\pi\delta\left[|q^0| - \frac{\mathbf{q}^2}{2m}\right]\rho \,. \tag{2.16}$$

By means of this approximation one can immediately evaluate (2.15) for $p^0=\mu$, $\mathbf{p}=\mathbf{0}$. One will have the following integral:

$$\int d\omega'\delta\left[\omega' - \frac{\mathbf{q}^2}{2m}\right]\delta\left[p^0-\omega' - \frac{\mathbf{q}^2}{2m}\right] = \delta\left[p^0 - \frac{\mathbf{q}^2}{m}\right] . \tag{2.17}$$

Hence,

$$\omega' = q^0 = \frac{\mathbf{q}^2}{2m} = \frac{p^0}{2} \,, \tag{2.18}$$

which gives us the δ of conservation of energy for the case where the pion energy goes into throwing two particles to the continuum with momentum $\mathbf{q}$. (This has come about because of the limit of zero momentum for the holes in Fig. 2, which is equivalent for this purpose to assuming static nucleons in the Fermi sea.) It also shows that the pion energy is equally shared between the two particle-hole excitations (in this approximation) and that the energy transferred by the virtual pion is $p^0/2$. These approximations, which have been used in previous works,[28,29] appear naturally and in an obvious way in the present context when one uses the low density limit of Eq. (2.16).

Explicit calculation of (2.15) gives, in the present case,

$$\mathrm{Im}\Pi(p^0,\mathbf{p}=\mathbf{0}) = -4\pi\frac{f^2(q^2)}{\mu^2}\rho^2 m\bar{q}\,{}^3D_0^2(q^0,\bar{q})\left[\left[\frac{2\lambda_1}{\mu}\right]^2 + 2\left[\frac{\lambda_2}{\mu^2}(p^0+q^0)\right]^2\right]\Bigg|_{q^0=p^0/2,\ \bar{q}=(mp^0)^{1/2}} \,, \tag{2.19}$$

where $\bar{q}$ is given by (2.17),

$$\bar{q} = (mp^0)^{1/2} \,. \tag{2.20}$$

By means of (1.1) we can write the value of $\mathrm{Im}B_0$,

$$2p^0\mathrm{Im}V_{\mathrm{opt}} = \mathrm{Im}\Pi = -4\pi\left[1+\frac{\epsilon}{2}\right]\mathrm{Im}B_0\rho^2 \,. \tag{2.21}$$

Hence,

$$\mathrm{Im}B_0 = \frac{1}{1+\epsilon/2}\frac{f^2(q^2)}{\mu^2} m\bar{q}\,{}^3D_0^2(q^0,\bar{q})\left[\left[\frac{2\lambda_1}{\mu}\right]^2 + 2\left[\frac{\lambda_2}{\mu^2}(p^0+q^0)\right]^2\right]\Bigg|_{q^0=p^0/2} \,. \tag{2.22}$$

by using $f^2/4\pi=0.08$ and the values for λ_1 and λ_2 through Eqs. (1.2) and (2.3) ($\lambda_1=0.0075$, $\lambda_2=0.053$), we obtain

$$\mathrm{Im}B_0=0.021\mu^{-4} . \tag{2.23}$$

Thus we get similar results to those in Ref. 29, and about a factor of 2 low compared with the empirical values.

We cannot get such a similar analytical expression for the real part of B_0 in the same limit, but a numerical evaluation of (2.13) gives

$$\mathrm{Re}B_0=-0.0042\mu^{-4} , \tag{2.24}$$

which comes approximately in equal parts from the real background in the Wick rotation and the pole term [second term in (2.13)]. This sign is different from other approaches, but this should be less surprising after what we said in the Introduction. The fact that we include some crossed terms by means of the full Lindhard function is partly responsible for this sign.

This value of $\mathrm{Re}B_0$ is, however, only a piece, and not the most important of the total $\mathrm{Re}B_0$. As we shall see, most of the contributions come from other diagrams that involve Δh excitations. In addition to this new diagram, which contributes to the real part of B_0, we will also consider exchange terms to the one considered up to now, which also contribute to the imaginary part, helping to improve the agreement of $\mathrm{Im}B_0$ with the empirical values.

III. EXCHANGE AND Δ TERMS

Let us now consider the diagram of Fig. 3, which replaces the ph excitation of the pion in Fig. 2 by a Δh. The formalism that we are using allows for immediate inclusion of this piece. All one has to do is to substitute for $U_N(q)$ by $U_\Delta(q)$ in (2.14), where $U_\Delta(q)$ is the Lindhard function for Δh excitation.[36,37,39,41]

For the $\Delta N\pi$ vertex one takes a phenomenological Hamiltonian given in momentum space by

$$\delta\tilde{H}_{\pi N\Delta}=i\frac{f^*}{\mu}\langle m_s \mid \mathbf{S}\cdot\mathbf{q} \mid M_s\rangle\langle m_t \mid T^\lambda \mid M_t\rangle , \tag{3.1}$$

corresponding to the vertex of Fig. 8. The Δh Lindhard function has to be correspondingly normalized to match the definition of U_N in (2.7). With this normalization the pion self-energy due to ph excitation is given by

$$\Pi_N^0(q)=\frac{f^2(q^2)}{\mu^2}\mathbf{q}^2U_N(q) . \tag{3.2}$$

Thus we will define $U_\Delta(q)$ such that

$$\Pi^0(q)=\frac{f^2(q^2)}{\mu^2}\mathbf{q}^2[U_N(q)+U_\Delta(q)] , \tag{3.3}$$

with

$$U_\Delta(q)=\frac{16}{9}\left[\frac{f^*}{f}\right]^2\int\frac{d\mathbf{k}}{(2\pi)^3}\left[\frac{n(\mathbf{k})}{q^0+\varepsilon(\mathbf{k})-\omega_R-\varepsilon_\Delta(\mathbf{k}+\mathbf{q})+i(\Gamma(k+q)/2)}+\frac{n(\mathbf{k})}{-q^0+\varepsilon(\mathbf{k})-\omega_R-\varepsilon_\Delta(\mathbf{k}-\mathbf{q})+i(\Gamma(k-q)/2)}\right] , \tag{3.4}$$

where $\omega_R=m_\Delta-m_N$, and $\Gamma(q)$ is the free width of the Δ, which is zero for the arguments that we need in this problem. The two terms of (3.4) correspond to the direct and crossed Δh excitations exhibited in Fig. 9. Equation (3.4) can be integrated and explicit expressions can be found in Refs. 39 and 41.

A low density approximation of (3.4) immediately gives for positive q^0

$$U_\Delta(q)=\frac{4}{9}\left[\frac{f^*}{f}\right]^2\left[\frac{\rho}{q^0-\omega_R-\mathbf{q}^2/2m_\Delta+i\Gamma(q)/2}+\frac{\rho}{-q^0-\omega_R-\mathbf{q}^2/2m_\Delta}\right] . \tag{3.5}$$

We can get an estimate of the real part of (2.13) due to ph or Δh excitation. For this purpose we will take the second term in (2.13) and evaluate the Lindhard functions in an average point of the integrand, which for simplicity can be taken to be the same as that which gives rise to the imaginary part in the low density approximation, Eqs. (2.17)–(2.19). A direct evaluation of $U_N(q)$ gives

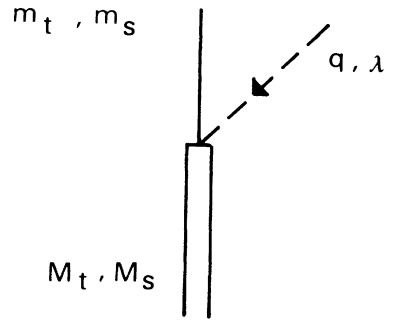

FIG. 8. Vertex of the $\pi N\Delta$ interaction.

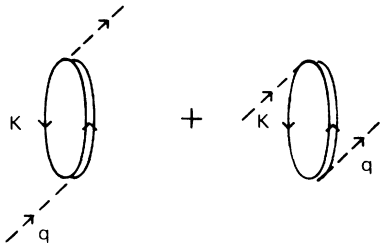

FIG. 9. The Lindhard function representation for the Δh excitation. Direct and crossed terms.

$$\mathrm{Re}U_{\mathrm{N}}\left[q^0=\frac{p^0}{2}=\frac{\bar{q}^{\,2}}{2m},\bar{q}\right]=-\frac{m}{\bar{q}^{\,2}}\rho,\quad \rho\to 0\ . \tag{3.6}$$

Actually, we can identify the result in (3.6) with the crossed term [second term in (2.9) in the limit of $\rho\to 0$]. This shows a peculiar characteristic of the Lindhard function. The direct term [first term in (2.9)] changes sign precisely at $q^0=\mathbf{q}^2/2m$ in the low density limit, as can be seen directly from (2.9), with $\mathrm{Re}U_{\mathrm{N}}>0$ for $q^0>\mathbf{q}^2/2m$ and $\mathrm{Re}U_{\mathrm{N}}<0$ for $q^0<\mathbf{q}^2/2m$. One should then expect large cancellations in that integral, which appears to be the case, with a small contribution to $\mathrm{Re}B_0$ from this source. On the other hand, $U_{\Delta}(q)$ has a sizable magnitude $[U_{\Delta}(q)\approx 2U_{\mathrm{N}}^{\mathrm{crossed}}(q)]$ and has the same negative sign over the entire integration domain. Thus, the contribution to $\mathrm{Re}B_0$ from the Δh excitation piece can be appreciable. When actual calculations are carried out, one obtains

$$\begin{aligned}\mathrm{Re}B^{\Delta}_{0,\mathrm{back}}&=0.0012\mu^{-4}\ ,\\ \mathrm{Re}B^{\Delta}_{0,\mathrm{pole}}&=0.054\mu^{-4}\ ,\\ \mathrm{Re}B^{\Delta}_{0}&=0.055\mu^{-4}\ ,\end{aligned} \tag{3.7}$$

where the background and the pole part of $\mathrm{Re}B_0$ correspond to the first and second terms in Eq. (2.13). The Δ term gives a sizable contribution to $\mathrm{Re}B_0$, of the order of $\mathrm{Im}B_0$ and of the same sign.

We would like to calculate the exchange part of the diagrams in Figs. 2 and 3. These diagrams are now depicted in Fig. 10. The explicit calculation of the diagrams is technically more involved and the details can be seen in Ref. 46.

We recall here the results in the low density limit. From the diagram of Fig. 10(a), we get

$$\mathrm{Im}B_0=\frac{1}{1+\epsilon/2}\frac{f^2(q^2)}{\mu^2}m\bar{q}\,{}^3D_0^2(q^0,\bar{q})\times\left[\frac{\lambda_1}{\mu}\frac{\lambda_2}{\mu^2}(2p^0+2q^0)-\left[\frac{\lambda_1}{\mu}\right]^2\right]\Bigg|_{q^0=p^0/2}\ , \tag{3.8}$$

with the same values for $\bar{q}$ and q^0 as in Eq. (2.19). Analogously, from Fig. 10(b), we get

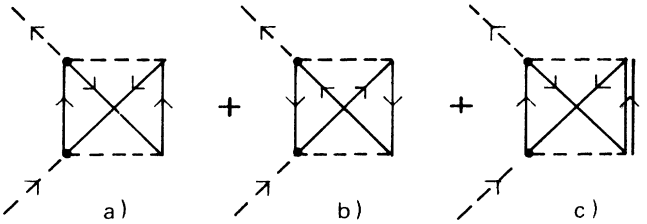

FIG. 10. Exchange terms of Figs. 2 and 3.

$$\mathrm{Im}B_0=\frac{1}{1+\epsilon/2}\frac{f^2(q^2)}{\mu^2}m\bar{q}\,{}^3D_0^2(q^0,\bar{q})\times\left[\frac{\lambda_1}{\mu}\frac{\lambda_2}{\mu^2}(2p^0+2q^0)+\left[\frac{\lambda_1}{\mu}\right]^2\right]\Bigg|_{q^0=p^0/2}\ . \tag{3.9}$$

On the other hand, the diagram of Fig. 10(c) does not contribute to the imaginary part.

As one can see from (3.8) and (3.9), there is a cancellation of the term with $(\lambda_1/\mu)^2$ when both diagrams are added. We will present, in what follows, results relating to exchange terms as the sum of the contribution from both diagrams. Hence,

$$\mathrm{Im}B_0^{\mathrm{ex}}=\frac{1}{1+\epsilon/2}\frac{f^2(q^2)}{\mu^2}m\bar{q}\,{}^3D_0^2(q^0,\bar{q})3p^0\frac{2\lambda_1}{\mu}\frac{\lambda_2}{\mu^2}\ , \tag{3.10}$$

which has the numerical value

$$\mathrm{Im}B_0^{\mathrm{ex}}=0.004\mu^{-4}\ . \tag{3.11}$$

Hence, the exchange terms introduce a 20% increase in $\mathrm{Im}B_0$, which now has the value $0.025\mu^{-4}$, still low compared to the empirical numbers.

With respect to the real part, a numerical calculation in the low density limit for the sum of the nucleon exchange graphs gives

$$\begin{aligned}\mathrm{Re}B^{\mathrm{N\,ex}}_{0,\mathrm{back}}&=-0.0008\mu^{-4}\ ,\\ \mathrm{Re}B^{\mathrm{N\,ex}}_{0,\mathrm{pole}}&=-0.0024\mu^{-4}\ ,\\ \mathrm{Re}B^{\mathrm{N\,ex}}_{0}&=-0.0032\mu^{-4}\ .\end{aligned} \tag{3.12}$$

Once again the real part coming from the Δ exchange graph from Fig. 10(c) gives a larger contribution to $\mathrm{Re}B_0$ than the nucleon part, and one gets

$$\begin{aligned}\mathrm{Re}B^{\Delta\,\mathrm{ex}}_{0,\mathrm{back}}&=0.004\mu^{-4}\ ,\\ \mathrm{Re}B^{\Delta\,\mathrm{ex}}_{0,\mathrm{pole}}&=-0.015\mu^{-4}\ ,\\ \mathrm{Re}B^{\Delta\,\mathrm{ex}}_{0}&=-0.011\mu^{-4}\ .\end{aligned} \tag{3.13}$$

Thus, with all the diagrams included, in the limit of low densities one obtains

$$\begin{aligned}\mathrm{Im}B_0&\approx 0.025\mu^{-4}\ ,\\ \mathrm{Re}B_0&\approx 0.037\mu^{-4}\ .\end{aligned} \tag{3.14}$$

The low density limit considered here has allowed us to do simple analytical calculations for the imaginary parts, or easy numerical calculations for the real part,

increasing our understanding of the problem. In spite of the more elaborate calculations that will be done later, the results in (3.14) give the correct order of magnitude and can be considered as approximate results.

IV. PAULI EXCLUSION EFFECTS

The approximate calculations carried out so far do not consider the Pauli exclusion principle. Indeed, the approximation for $\mathrm{Im}U_N$ in (2.16) has neglected the factor $1-n(\mathbf{k}+\mathbf{q})$, which forces the particle line in the ph excitation, with momentum $\mathbf{k}+\mathbf{q}$, to be above the Fermi sea.

The consideration of these effects does not offer any particular problem in the approach. All one has to do is to systematically use the nucleon propagators of Eq. (2.8). The calculation of the direct graphs, Figs. 2 and 3, the most important for both $\mathrm{Re}B_0$ and $\mathrm{Im}B_0$, is particularly simple since the nucleon medium propagators get factorized by means of the Lindhard function, which takes care properly, in any exact way, of the Pauli exclusion principle. Hence, one can evaluate Eq. (2.13) with U_N or U_Δ in (2.14) by means of the exact expressions for U_N and U_Δ, Refs. 39–41, and the Pauli exclusion principle is automatically taken into consideration. If we do so, we obtain the results shown in Fig. 11 for $\mathrm{Im}B_0$ as a function of the nuclear density. One can appreciate there the remarkable constancy of $\mathrm{Im}B_0$ as a function of ρ, which gives support to calculations done in the low density limit. For $\rho=\rho_0(0.483\mu^3)$, one gets a reduction of about 15% with respect to the calculation at $\rho=0$.

The results are quite different for the real parts. If we take as a reference the direct Δ term of Fig. 3, the pole part of $\mathrm{Re}B_0^{\Delta,d}$ shows a rapid decrease as a function of ρ, which can be appreciated in Fig. 12. A similar behavior can be seen for $\mathrm{Re}B_0^{\Delta\,ex}$, the exchange Δ graph shown in Fig. 10(c).

For the real part of the nucleon terms, direct and exchange, the trend is similar and there is a reduction in the size of the contribution, although more moderate than in the Δ case. The sum of all the contributions for $\mathrm{Re}B_0$ shows similar characteristics. It decreases quite fast for small values of ρ and then stabilizes to a constant in a broad range of densities. The background part of the direct Δ term is, however, remarkably constant.

The results in Fig. 12 clearly show the relevance of the Pauli excitation principle in this type of calculation. Indeed, the value for $\mathrm{Re}B_0$ which we would choose, at $\rho\approx 0.5\rho_0$, is about $\frac{2}{3}$ of the value at $\rho=0$.

It is quite instructive to look at the reasons for such

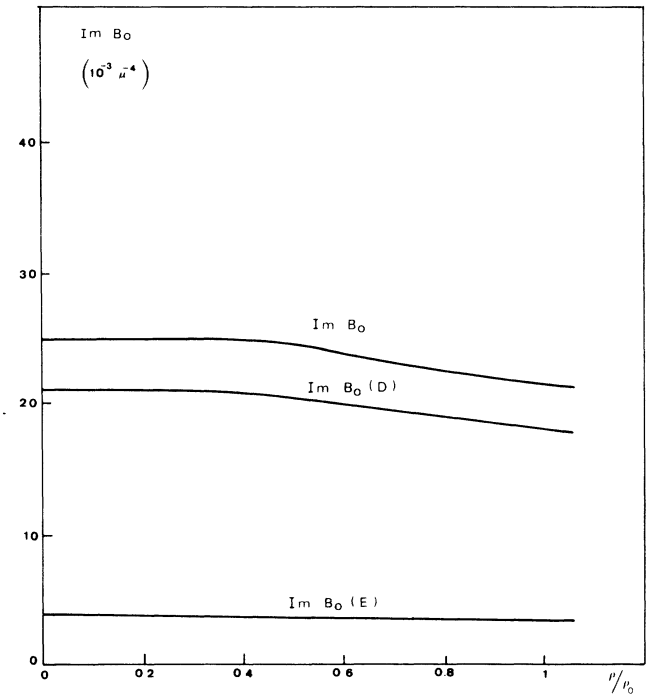

FIG. 11. The imaginary part of the B_0 parameter as a function of the nuclear density. $\mathrm{Im}B_0^d$ comes from the direct term, Fig. 2, $\mathrm{Im}B_0^{ex}$ from the exchange term, Fig. 10, and $\mathrm{Im}B_0$ from the sum of the two terms. (No off-shell effects, no correlations, and no pion polarization are included.)

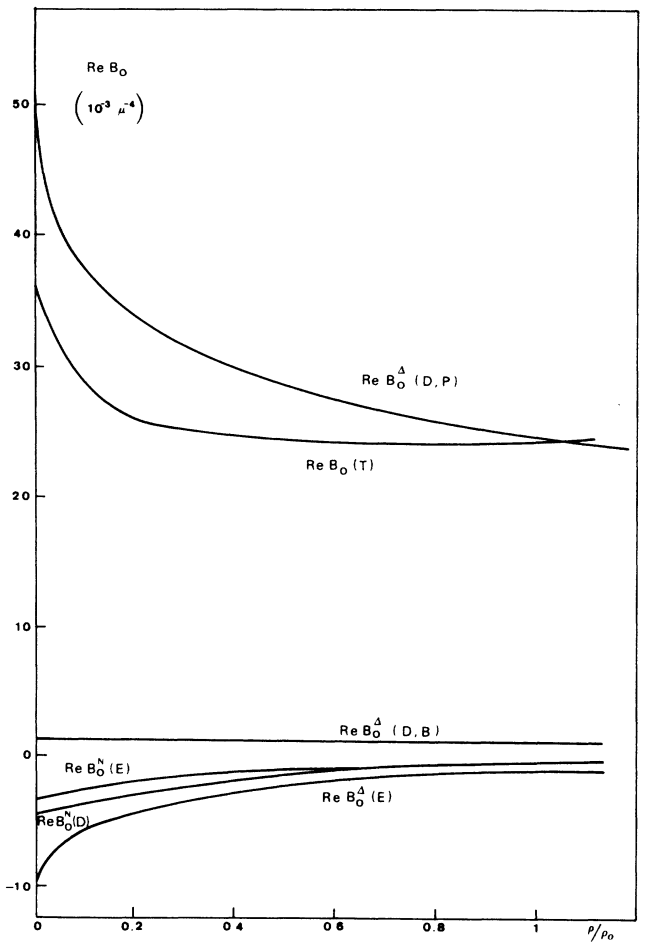

FIG. 12. The real part of B_0 for the same case as in Fig. 11. $\mathrm{Re}B_0^N$ or $\mathrm{Re}B_0^\Delta$ indicate contribution from ph-ph excitation or ph-Δh excitation. DP: direct term (Fig. 3), pole part of the Wick rotation. DB: direct term, background part from the Wick rotation. E: exchange term (Fig. 10). D: direct. T: total.

peculiar behavior. We know that $\mathrm{Re}U_N(q)$ is not affected by the Pauli exclusion principle. The same happens to $U_N(q)$ for complex values of q^0.

On the contrary, $\mathrm{Im}U_N(q)$ is appreciably affected by the Pauli exclusion principle. In Eq. (2.16) we obtained an approximation by disregarding the $n(\mathbf{k})n(\mathbf{k}+\mathbf{q})$ term in (2.9). We can now do a better approximation by neglecting the $(\mathbf{k}\cdot\mathbf{q})/m$ term in the denominator of (2.9), but keeping the product $n(1-n)$. This immediately leads to the result

$$\mathrm{Im}U_N(q) \underset{\rho\to 0}{\approx} -\pi\rho\delta(|q^0|-\varepsilon(\mathbf{q})) \times\left[1-\theta(2-\tilde{q})\left[1-\tfrac{3}{4}\tilde{q}+\frac{\tilde{q}^3}{16}\right]\right], \quad (4.1)$$

where $\tilde{q}=|\mathbf{q}|/k_F$. Equation (4.1) is a sensible improvement over (2.16) and gives rise to results very similar to those obtained with the exact value of $\mathrm{Im}U_N$ when used inside an integral.

If we now evaluate the imaginary part of $\Pi(p)$ through Eq. (2.15), we will need

$$\mathrm{Im}U_N(\omega',\mathbf{q})\mathrm{Im}U_N(p^0-\omega',\mathbf{q}) \quad (\text{at } \mathbf{p}=\mathbf{0}) .$$

Because of the δ function in (4.1), we still have the same integration as in (2.17) which fixes ω', q^0, and $\mathbf{q}^2/2m$ to the value $p^0/2$ as before. Since $\mathbf{q}$ is fairly large, the effects of the Pauli correction are not too large. Even at $\rho=\rho_0$ one has $\tilde{q}=1.35$ and the correction to $\mathrm{Im}U_N$ from (4.1) is only of 15%. This justifies the fact that the Pauli exclusion effect in $\mathrm{Im}B_0$ is not too important, as we have seen in Fig. 11.

However, if we evaluate the real part of $\Pi(p)$, things are rather different. Indeed, let us concentrate on $\Pi^\Delta(p)$, which gives the largest contribution to the real part of B_0. The real part now comes from Eq. (2.13) after substituting for $U_N(q)$ in (2.14) by $U_\Delta(q)$. The contribution of the real background [Euclidean contribution from Wick rotation or first term in (2.13)] is not affected by the Pauli exclusion principle since it involves only the Lindhard function $U_N(q)$ for complex values of q^0, where the Pauli exclusion is inoperative. The contribution from the pole term [second term in (2.13)] now requires $\mathrm{Im}U_N(\omega',q)$, where the Pauli exclusion effect is operative.

One can actually evaluate analytically the integral in (2.13) by using Eq. (4.1) (we ignore, for simplicity, the πNN form factor, which does not play an important role here because of the limited range of integration). After a few approximations one obtains

$$\mathrm{Re}B_0^{\Delta,\mathrm{pole}}=0.050\mu^{-4}-0.019k_F\mu^{-5} . \quad (4.2)$$

The value $0.050\mu^{-4}$ at $\rho=0$ is in fair agreement with the more accurate calculation of Eq. (3.7). The fact that the Pauli correction goes as k_F, rather than as k_F^3, makes the correction more considerable. The fact that the $\mathbf{q}^2$ power of the phase space $d\mathbf{q}$, as well as the other $\mathbf{q}^2$ power in the integrand, are cancelled by the pion propagators is the essential element responsible for the k_F dependence. At $\rho=\rho_0/10$, $k_F=0.90\mu$ and the Pauli correction subtracts around $0.017\mu^{-4}$ from the $\rho=0$ value of $\mathrm{Re}B_0^{\Delta,\mathrm{pole}}$. This is also in fair agreement with the more elaborate calculation of Fig. 12.

The calculations carried out in this section and their discussion have served to stress the role of the Pauli principle in such calculations and the need to consider it properly when evaluating the real part of the optical potential.

An alternative approach to the one followed here, which is particularly useful to avoid double counting diagrams, is shown in Appendix A, where the second order Pauli corrected term is derived and a critical discussion of higher order corrections in connection with it is done.

V. OFF-SHELL EFFECTS

We have already introduced the off-shell dependence of the p-wave πNN coupling in Sec. II through a monopole form factor, Eq. (2.10). But up to now we have not considered the off-shell extrapolation of the s-wave πN amplitude.

The off-shell extrapolation of the s-wave amplitude requires some extra attention. The virtual pions which appear in the calculation of $\mathrm{Im}\Pi(p)$ have $q^0\simeq\mu/2$ and $|\mathbf{q}|\simeq\sqrt{\mu m}$. The real part meets with pions that essentially go from the on-shell situation [when $\omega'=0$, $q^0=p^0$, $\mathbf{q}=0$ in (2.13)] to off-shell situations with $q^0=0$, $|\mathbf{q}|=\sqrt{2m\mu}$, if we take the pole part of (2.13) as a reference. An off-shell extrapolation that starts from the on-shell value at threshold and extrapolates the results to the situation found here would be appropriate to our problem.

In the spirit of dealing explicitly with the mesonic degrees of freedom, as we have done so far, we have also followed a mesonic exchange based model for the s-wave part of the amplitude, shown graphically in Fig. 13. Such an off-shell extrapolation has been used in a problem similar to that we have here, i.e., pion absorption in the deuteron and its reverse process, $pp\to d\pi^+$.[32]

In this model the off-shell dependence of the λ_2 parameter is given by the t dependence of the ρ meson propagator [$t=(q-q')^2$]. The off-shell dependence of

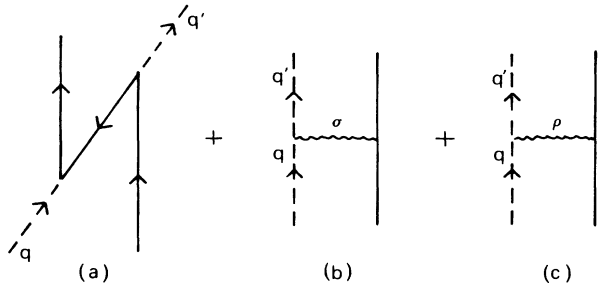

FIG. 13. Diagrammatic model of the s-wave πN scattering matrix. (a) Pair term, (b) σ-exchange term, and (c) ρ-exchange term.

the λ_1 parameter will be given by the t dependence of the σ propagator. One is implicitly assuming that the vertices involved in Fig. 13 are of shorter range than the range given by the inverse mass of the meson masses. Because of the large mass of the $NN\bar{N}$ intermediate state in the pair term, this piece will have a short range and can be approximately taken as constant; hence the λ_1 part will contain a constant background and the σ term, while the λ_2 part of the interaction will contain the ρ meson piece of Fig. 13. The off-shell extrapolation is then straightforward and one has[32]

$$\lambda_1(t)=-\tfrac{1}{2}(1+\epsilon)\mu\left[a_{\rm SR}+a_\sigma\frac{m_\sigma^2}{m_\sigma^2-t}\right],$$
$$\lambda_2(t)=\lambda_2\frac{m_\rho^2}{m_\rho^2-t}, \tag{5.1}$$

where $a_\sigma=0.220\mu^{-1}$ (Ref. 47), $m_\rho=770$ MeV, $m_\sigma\simeq 550$ MeV, and $a_{\rm SR}=-0.233\mu^{-1}$ to match λ_1 on shell. The parameter λ_1 shows the cancellation at $t=0$, as required by PCAC, and provides larger values of $\lambda_1(t)$ if one goes to situations with $t<0$.

We have performed the calculations by using Eq. (5.1) for consistency with the pion absorption in the deuteron[32] worked out with the same model. The results using other off-shell extrapolations, shown in Appendix B, do not differ much from this one.

In Fig. 14 we plot the results of the different off-shell extrapolations in the λ_1 parameter. The label LMM stands for the extrapolation of Ref. 64 [Eq. (B4)], that called PCAC stands for Refs. 60, 61, and 63 [Eqs. (B1)–(B3)], while that labeled Hamilton stands for the off-shell extrapolation of Eq. (5.1).

We can easily check the influence of the off-shell extrapolation on the imaginary part of B_0 in the low density limit that we used in Sec. II. Indeed, by means of the fixed kinematics in (2.18), and substituting for λ_1,λ_2 by $\lambda_1(t),\lambda_2(t)$ of (5.1) in Eq. (2.22), we have (at $\mathbf{p}=\mathbf{0}$)

$$\mathrm{Im}B_0^d=0.027\mu^{-4}. \tag{5.2}$$

Hence $\mathrm{Im}B_0^d$ has not changed much after all these ingredients have been introduced. The small effect of all these corrections is due to cancellation among different effects. By means of (5.1), $\lambda_1(t)$ appreciably increases its value with respect to $\lambda_1(0)$ and the factor $\lambda_2(t)$ is slightly reduced. Altogether, the net effect is small, as we said.

The situation is different, however, in the exchange term studied in Sec. III. Indeed, the contribution to $\mathrm{Im}B_0$ from those terms, given in Eq. (3.10), is proportional to $\lambda_1\cdot\lambda_2$, and, as we said, λ_1 was increased more effectively than λ_2 was decreased, such that this piece gets appreciably modified. By using the same kinematics as we used before, we now obtain

$$\mathrm{Im}B_0^{\rm ex}=0.019\mu^{-4}. \tag{5.3}$$

Thus the total value of $\mathrm{Im}B_0$ from the direct and exchange terms is now

$$\mathrm{Im}B_0=0.046\mu^{-4}, \tag{5.4}$$

which shows a 70% increase with respect to the $0.025\mu^{-4}$ value that we had before and is in much better agreement with the empirical results, although, as we shall see immediately, the effect of short-range correlations will kill much of this enhancement.

With respect to the real parts, we now get for the direct terms, also at $\rho=0$,

$$\mathrm{Re}B_{0,\rm back}^d=0.041\mu^{-4},$$
$$\mathrm{Re}B_{0,\rm pole}^d=0.067\mu^{-4}, \tag{5.5}$$
$$\mathrm{Re}B_0^d=0.108\mu^{-4},$$

and, for the exchange terms,

$$\mathrm{Re}B_{0,\rm back}^{\rm ex}=-0.007\mu^{-4},$$
$$\mathrm{Re}B_{0,\rm pole}^{\rm ex}=-0.020\mu^{-4}, \tag{5.6}$$
$$\mathrm{Re}B_0^{\rm ex}=-0.027\mu^{-4}.$$

Hence the total contribution to $\mathrm{Re}B_0$ is given by

$$\mathrm{Re}B_0=0.081\mu^{-4}. \tag{5.7}$$

As was the case before, the Δ term in the direct and exchange terms gives the largest contribution to (5.5) and (5.6). If we compare these results with those in (3.14), we see that the imaginary part of B_0 has increased by about 70%, while $\mathrm{Re}B_0$ has been modified by about 100%.

Another ingredient that should be considered here is the effect of short-range correlations in cutting the contribution from small distances or conversely from large momenta. Such effects have been considered on other occasions[29] and show very small corrections for $\mathrm{Im}B_0$ but larger corrections in $\mathrm{Re}B_0$. We will implement the corrections in momentum space. For this purpose we

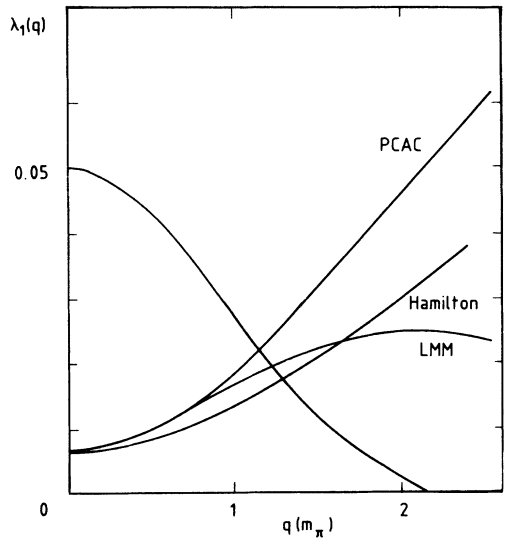

FIG. 14. Different off-shell extrapolations of the isoscalar s-wave amplitude. PCAC: from Refs. 59–61 and 63. Hamilton: from Ref. 47. LMM: from Ref. 64. The unlabeled curve is $\tilde{\rho}(q)$, the Fourier transform of the ^{16}O density with arbitrary normalization, shown for comparison purposes.

will use a correlation function in coordinate space, which is simple enough to allow for analytical calculations and allows one to account approximately for the effects of more realistic correlation functions.

We take

$$g(r)=1-j_0(q_c r)\ , \tag{5.8}$$

where q_c is the inverse of the range of the short range correlations. With the value of $q_c \approx m_\omega$, Eq. (5.8) shows an appreciable similarity to more realistic correlation functions.[48,49]

By following steps similar to those of Ref. 49, we find that the potential in momentum space, $V(q)$, coming from a pion exchange with an s-wave vertex and a p-wave vertex,

$$V(q)=\frac{f}{\mu}v_\pi(q^2)q_i\sigma_i\tau^\lambda\ , \tag{5.9}$$

is changed to

$$\tilde{V}(q)=\frac{f}{\mu}[v_\pi(q^2)-\tilde{v}_\pi(q^2)]q_i\sigma_i\tau^\lambda\ , \tag{5.10}$$

where $\tilde{v}_\pi(q^2)\equiv v_\pi(q^2-q_c^2)$. We introduce the short-range correlations according to the prescription of changing (5.9) by (5.10) and we obtain, at $\rho=0$,

$$\begin{aligned}&\mathrm{Im}B_0=0.031\mu^{-4}\ ,\\ &\mathrm{Re}B_0=0.041\mu^{-4}\ .\end{aligned} \tag{5.11}$$

Thus, the effect of correlations is a decrease of 40% in $\mathrm{Im}B_0$ and a reduction of a factor of 2 in $\mathrm{Re}B_0$. The short-range correlations are effective in cutting down the contribution from large momentum transfers and thus make the final results less sensitive to the off-shell extrapolation than in the case where the correlations are not considered. The results in (5.11) are very similar to those obtained in (3.14) before off-shell effects and correlations were introduced.

The static correlation function of Eq. (5.8) is obviously an approximation to a more microscopic dynamical correlation function. It provides a fair approximation in the sense that it cuts the contribution of short distances in a realistic range of the repulsive forces. This is so much better for the long-range part of the potential as the pion exchange that we are considering here. The effective forces obtained by means of this simple correlation function compare very well with G-matrix calculations even for nonstatic situations (q^0 and $\mathbf{q}$ exchange) as the ones found here.[50] In any case we shall comment later on the changes of the results brought up by reasonable changes of this correlation function, which can give us an idea of the theoretical uncertainties of our calculation.

With respect to the density dependence of $\mathrm{Re}B_0$ and $\mathrm{Im}B_0$, we show the results in Fig. 15 (dashed lines) and Fig. 16. Figure 15 shows in dashed lines the results for $\mathrm{Im}B_0$. As we saw before in Fig. 11, there is some reduction at finite densities with respect to the results at $\rho=0$, due to the effect of the Pauli exclusion principle (studied in Sec. IV). The reduction is moderate, however, in

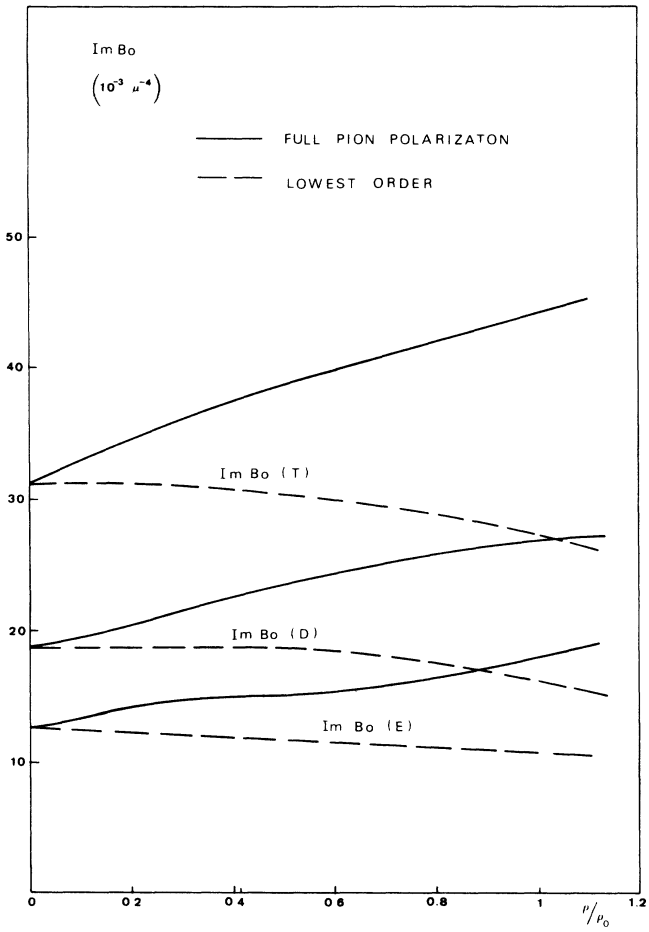

FIG. 15. Density dependence of $\mathrm{Im}B_0$, calculated with the inclusion of off-shell effects, form factor, and short-range correlations. *Dashed lines:* the calculations here only include the polarization of the pion in lowest order. D: direct (graphs of Fig. 2). E: exchange [graphs of Figs. 10(a) and 10(b)]. T: total. We refer to this calculation as lowest order in future figures. *Solid lines:* Density dependence of $\mathrm{Im}B_0$ when, in addition to the off-shell extrapolation and short-range correlations, we consider the full polarization of the pion.

$\mathrm{Im}B_0$. In contrast, Fig. 16 shows the important reduction due to the Pauli effect in $\mathrm{Re}B_0$. In Fig. 16 we can see the contribution of the different parts of $\mathrm{Re}B_0$. The comments are much the same as those exposed in Sec. IV and we omit their repetition here. We only mention that proper consideration of the Pauli exclusion principle here leads to a 20–25 % reduction of $\mathrm{Re}B_0$ when all contributions are added. The reduction in size, $\Delta\,\mathrm{Re}B_0\simeq-0.010\mu^{-4}$, is about the same as that found in Fig. 12.

For values of $\rho\simeq(0.5-0.65)\rho_0$ as found in Refs. 14 and 18 for the effective density, one obtains values of $\mathrm{Re}B_0\simeq0.031\mu^{-4}$ and $\mathrm{Im}B_0\simeq0.030\mu^{-4}$. The value for $\mathrm{Im}B_0$ is a little low compared with the empirical results of Eq. (1.4). On the other hand, $\mathrm{Re}B_0$ has an opposite sign to that we assume as the best fit parameter in Eq. (6.11).

As we shall see in the next section, including higher order terms to account for pion polarization in the medi-

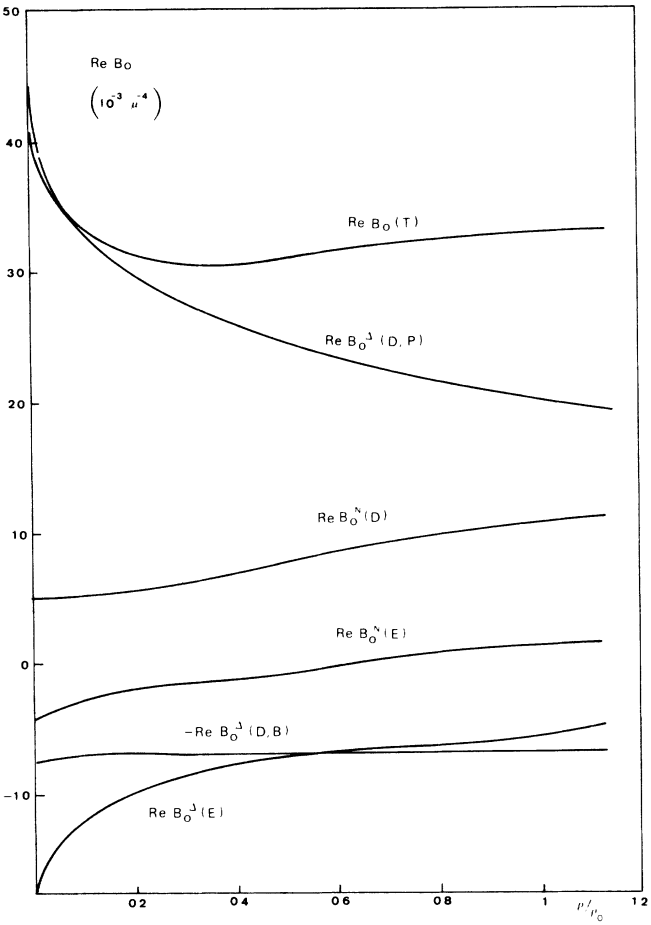

FIG. 16. Density dependence of $\mathrm{Re}B_0$, with pion polarization in lowest order, but including off-shell effects and short-range correlations. The notation is the same as in Fig. 12.

um produces an appreciable enhancement in $\mathrm{Im}B_0$ that makes our results much closer to the empirical ones. On the other hand, the real part is not affected much and has about the same value, with opposite sign to the one which we will quote as the best fit value in Eq. (6.11). However, as we shall see in Sec. VII, the off-shell effects considered here have also some repercussions in the first order optical potential parameter b_0, owing to which the results quoted in (6.11) have to be modified.

VI. HIGHER ORDER CONTRIBUTIONS

We now turn to consider higher order corrections from the polarization of the pion propagator. This corresponds to the diagrams implicit in Fig. 4. We have pointed out before the importance of dressing up properly the pion propagator in the medium, essentially because of the small mass of the pion, which makes the pion self-energy comparable or sometimes much larger than the squared pion mass. Thus Figs. 2 and 3 can be considered as the first term of the series implicit in Fig. 4, which contains the iterated ph and Δh excitation that gives rise in the first order response function of the medium to the pion source.[36]

In Fig. 4 we have drawn wavy lines to connect the ph or Δh components. While the explicit consideration of the πN s-wave amplitude that we are doing forces a pion to attach to the s-wave vertices, the p-wave interaction between different particle hole components allows for more ingredients. This interaction in the $T=1$ channel contains π exchange, and ρ exchange, and both are modified by the effect of short-range correlations in the same way as in the former section. This is done in detail in Refs. 49 and 41 and leads to a ph interaction which can be written as

$$\tilde{V}_{\mathrm{ph}}(q)=[A(q)(\delta_{ij}-\hat{q}_i\hat{q}_j)+B(q)\hat{q}_i\hat{q}_j]\sigma_i\sigma_j\tau\tau\ , \tag{6.1}$$

where the coefficients A and B are given by

$$\begin{aligned} A(q)&=\frac{f^2}{\mu^2}[\mathbf{q}^2D_0^{\rho}(q)F_{\rho}^2(q)C_{\rho}-\tfrac{1}{3}q_c^2\tilde{D}_0^{\pi}(q)\tilde{F}_{\pi}^2(q)-(\mathbf{q}^2+\tfrac{2}{3}q_c^2)\tilde{D}_0^{\rho}(q)\tilde{F}_{\rho}^2(q)C_{\rho}]\ , \\ B(q)&=\frac{f^2}{\mu^2}[\mathbf{q}^2D_0^{\pi}(q)F_{\pi}^2(q)-(\mathbf{q}^2+\tfrac{1}{3}q_c^2)\tilde{D}_0^{\pi}(q)\tilde{F}_{\pi}^2(q)-\tfrac{2}{3}q_c^2\tilde{D}_0^{\rho}(q)\tilde{F}_{\rho}^2(q)C_{\rho}]\ , \end{aligned} \tag{6.2}$$

where D_0^{π},D_0^{ρ} are the pion or ρ meson propagator, F_{π},F_{ρ} the pion or ρ form factor,

$$C_{\rho}=(f_{\rho}^2/m_{\rho}^2)/(f_{\pi}^2/\mu^2)\approx 2\ ,$$

and $\tilde{X}(q^2)$ stands for $X(q^2-q_c^2)$. Here we use the same set of parameters that have been used in the study of a variety of physical phenomena by means of this effective interaction.[37] The part of (6.1) proportional to $A(q)$ is the transverse mode of propagation, while the term proportional to $B(q)$ takes care of the longitudinal propagation mode. Thus the ρ meson exchange is included in the term with A and the π meson exchange in the term with B.

By means of this interaction we can now sum up the full series involved in Fig. 4. With the nomenclature in Eqs. (5.9) and (5.10) we have, for the term of lowest order in density, the factor

$$\frac{f}{\mu}v_{\pi}(\mathbf{q}^2)q_i\frac{f}{\mu}v_{\pi}(\mathbf{q}^2)q_iU(q) \tag{6.3}$$

corresponding to a single ph or Δh excitation by the pion. Equation (6.3) formally accounts for the two s-wave vertices, the two pion propagators, and the ph or Δh excitation. The trace over spin and isospin has been included in $U(q)$. The full iteration of ph or Δh excitation will be taken into account by means of the series

$$\left[\frac{f}{\mu}\right]^2 v_\pi^2(\mathbf{q}^2)\mathbf{q}^2 U(q)\hat{q}_i\hat{q}_j\{\delta_{ij}+[A(q)(\delta_{ij}-\hat{q}_i\hat{q}_j)+B(q)\hat{q}_i\hat{q}_j]U(q)$$

$$+[A(q)(\delta_{il}-\hat{q}_i\hat{q}_l)+B(q)\hat{q}_i\hat{q}_l][A(q)(\delta_{lj}-\hat{q}_l\hat{q}_j)+B(q)\hat{q}_l\hat{q}_j]U^2(q)+\cdots\}\ . \tag{6.4}$$

One can immediately see that because of the orthogonality of the pion mode with the transverse mode, the terms with $A(q)$ vanish in (6.4) and one has the geometrical series

$$\left[\frac{f}{\mu}\right]^2 v_\pi^2(\mathbf{q}^2)U(q)\mathbf{q}^2[1+B(q)U(q)+B^2(q)U^2(q)+\cdots]=\left[\frac{f}{\mu}\right]^2 v_\pi^2(\mathbf{q}^2)U(q)\mathbf{q}^2\frac{1}{1-B(q)U(q)}\ . \tag{6.5}$$

Hence the difference with respect to the old calculation amounts to substituting

$$U(q)\rightarrow\frac{U(q)}{1-B(q)U(q)} \tag{6.6}$$

in Eq. (2.14). As we have already mentioned, if in (2.14) we substitute $U_N(q)$ by $U(q)$, containing the Lindhard function for ph and Δh excitation, and later on implement the change given by (6.6), we will be automatically considering the full induced interaction through both ph and Δh excitation.

With respect to the imaginary part of B_0 it is easy to estimate the effects of this medium renormalization. Indeed, we will now have in Eq. (2.15)

$$\mathrm{Im}U(q)\rightarrow\mathrm{Im}\left[\frac{U(q)}{1-B(q)U(q)}\right]=\frac{\mathrm{Im}U}{|1-BU|^2}\ . \tag{6.7}$$

Hence, in the limit of low densities where the kinematics is defined by Eq. (2.18), the results for $\mathrm{Im}B_0^d$ will be multiplied by the factor $|1-BU|^{-2}$. For the kinematical conditions of Eq. (2.18) one has $\mathrm{Re}U_N\approx-\rho$, $U_\Delta\approx-1.6\rho$, $\mathrm{Im}U_N\approx-1.5(\rho/\rho_0)^{2/3}$, and $B\approx-0.21$, all in pion units. At $\rho=\rho_0$ the renormalization factor in (6.7) introduces an increase of 60%. If one uses the effective density $\rho_{\mathrm{eff}}\approx\rho_0/2$ of Ref. 14, one has an increase of 30%.

These estimates compare extremely well with the exact calculations shown in Fig. 15. Around the values $\rho/\rho_0\approx0.5$–0.65, preferred as effective densities in Refs. 14 and 18, the values that we obtain for $\mathrm{Im}B_0$ are around

$$\mathrm{Im}B_0\approx(0.039-0.041)\mu^{-4} \tag{6.8}$$

which compare quite well with empirical estimates [$\mathrm{Im}B_0\simeq0.042\mu^{-4}$ in Ref. 14 in addition to other values quoted in Eq. (1.4)].

Similar polarization effects have been studied before, but considering only the pion polarization through Δh excitation.[51] Thus the part of the ph excitation is absent in the denominator of Eq. (6.7) and hence the interference of $\mathrm{Im}U_N$ between the numerator and denominator of Eq. (6.7) is lost.

By successive steps we have come to an expansion that looks like a standard expansion in powers of the nuclear density but, however, with the bare NN interaction substituted by the induced interaction.[40,52] This last is constructed in two steps: the first one sums ladder diagrams to correct for short distances (effect of the short-range correlations) and the second one excites iteratively ph (and Δh excitations in our case) to correct the long-range behavior of the interaction. Such a type of expansion appears naturally in other successful many-body schemes as the hypernetted chain expansion[53] and the planar theory.[54] The organizing principle in the expansion is then the number of ph excitations. The diagram of Fig. 4 would contain 2p-2h excitation in this scheme. A thorough study of terms with three-particle–three-hole excitation with the same expansion scheme, but for the p-wave part of the interaction, has been carried out in Ref. 5. The results show that at energies around resonance the three-body absorption mechanism can be compared to the two-body mechanism, but at energies around threshold the three-body mechanism becomes negligible compared with the two-body one. Since the phase space for the reaction is mostly responsible for these effects, we estimate that the three-body absorption mechanism is also small for the s-wave part, granting reasonable convergence of our expansion at the level of 2p-2h excitation. We expect the contribution from higher order to be of the same order or smaller than the theoretical errors from other sources as we shall comment later.

With respect to the real part of B_0 the density dependence is shown in Fig. 17. Comparison of the results with those of Fig. 16 in lowest order of the density shows that the real parts have not changed much when introducing the polarization of the pion. This situation has been found before in the evaluation of the Σ self-energy[55] and the Δ self-energy[18,4] in nuclear matter. This particular feature of the self-energy has to be attributed to the fact that the real parts get their contribution from large momenta, where the Lindhard function is much smaller (q^{-2} dependence asymptotically), and also one has the factor $(1-BU)^{-1}$ instead of $|1-BU|^{-2}$ that one has in the imaginary part.

From Fig. 17, and again for values of the density around $\rho\simeq(0.5$–$0.65)\rho_0$, we obtain

$$\mathrm{Re}B_0\approx(0.031-0.033)\mu^{-4}\ . \tag{6.9}$$

In the calculations of this section we have introduced all the elements that we have proven to be relevant in all

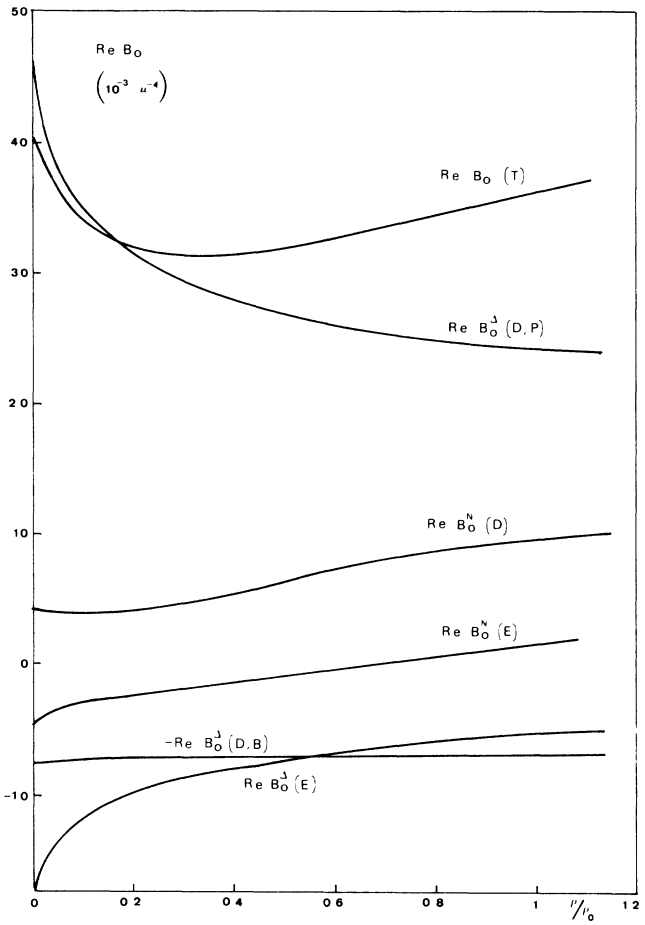

FIG. 17. Density dependence of $\mathrm{Re}B_0$ when the full pion polarization is included in addition to off-shell extrapolation and short-range correlations. The notation is the same as that in Figs. 12 and 16.

the previous sections, together with the higher order terms considered in this section. Thus the results in (6.8) and (6.9) are our ultimate results for B_0 which we again write below,

$$\begin{aligned} \mathrm{Im}B_0 &\approx (0.039-0.041)\mu^{-4}\ , \\ \mathrm{Re}B_0 &\approx (0.031-0.033)\mu^{-4}\ . \end{aligned} \tag{6.10}$$

The margins of errors quoted above are only because of the margin in ρ_{eff} that we have chosen. However, the calculation contains a certain number of parameters which are not exactly determined, although one does not have too much freedom with these parameters if one wishes to be consistent with other experiments, as we have pointed out. In order to have an idea of the theoretical uncertainties and the dependence of the results on the different parameter, we have made changes in the parameters and carried out the calculations. We can summarize the results as follows:

(a) An increase of q_c, the range parameter of the short-range correlations, by 10% increases $\mathrm{Re}B_0$ by about 13% and $\mathrm{Im}B_0$ by about 9%. In this last case the correlation effect is smaller because of the more limited range of momentum components allowed with respect to the case of $\mathrm{Re}B_0$. If q_c is decreased by a similar amount, the decrease in $\mathrm{Re}B_0$ and $\mathrm{Im}B_0$ is similar.

(b) In order to check the sensitivity to the off-shell extrapolation, we have changed m_σ in (5.1), which governs the increase of $\lambda_1(t)$ at $t<0$. We observe that a 10% increase in m_σ leads to a decrease of $\mathrm{Im}B_0$ and $\mathrm{Re}B_0$ by 10%. If m_σ is decreased by 10%, then $\mathrm{Re}B_0$ increases by about 11% and $\mathrm{Im}B_0$ increases by 13%. On the other hand, if we use the other off-shell extrapolations discussed in Appendix B, we can obtain variations at the level of 10–20 % for $\mathrm{Im}B_0$ and of 20–30 % for $\mathrm{Re}B_0$.

(c) The sensitivity to the form factor parameter Λ is not too important once short-range correlations are considered in addition. A change of 10% in the Λ in any direction leads to a 3% change of $\mathrm{Re}B_0$ and $\mathrm{Im}B_0$ in the same direction. Thus we can conclude that the results are rather stable and not strongly dependent on parameters which are not too precisely determined. The results are moderately sensitive to changes in the correlation function and in the off-shell extrapolation of the πN–s-wave amplitude, but rather independent of the πNN form factor.

In view of this dependence on the parameters and the uncertainties of these parameters allowed by other experiments that were used to fix them, a 20% theoretical uncertainty in the calculated values of $\mathrm{Im}B_0$ and 30% in $\mathrm{Re}B_0$ seem to us most likely.

In order to compare our results to the empirical fits, we shall take our value for b_0 ($b_0=-0.013\mu^{-1}$) together with the Pauli corrected rescattering term, Δb_0, of Appendix A ($\Delta b_0=-0.014\mu^{-1}$). Now we use the correlation found between the b_0 and the $\mathrm{Re}B_0$ parameters in the empirical fit of Ref. 14,

$$b_0+\alpha\,\mathrm{Re}B_0\approx\beta,\quad \alpha\approx 0.23\mu^3,\ \beta\approx -0.03\mu^{-1}$$

and we find, that by assuming $b_0=-0.027\mu^{-1}$ for the lowest part of the potential, the value of $\mathrm{Re}B_0$ that we would need to get a good fit to pionic atoms is

$$\mathrm{Re}B_0^{\mathrm{fit}}=-0.013\mu^{-4}\ . \tag{6.11}$$

There is an obvious discrepancy with the $\mathrm{Re}B_0$ from our calculations. This apparent discrepancy indicates that other effects come into way. The next section offers a look at a very important correction in the lowest order optical potential coming from off-shell extrapolations in the πN amplitude.

VII. INFLUENCE OF THE OFF-SHELL EXTRAPOLATION ON THE LOWEST ORDER PARAMETER

One aspect of our approach is that we make use of the local density approximation (LDA) to connect with the empirical optical potentials by performing our calculations in nuclear matter and then assuming that $\rho\to\rho(\mathbf{r})$, the nuclear density at a local point.

However, the strong off-shell dependence of the λ_1 parameter has immediate repercussions on the lowest order optical potential that go beyond the LDA approach. We shall investigate these effects in the present section.

The lowest order s-wave optical potential is given by

$$2\omega V_{\rm opt}^{(0)}(r) = -4\pi(1+\epsilon)[b_0\rho(r)+b_1(\rho_n(r)-\rho_p(r))] , \tag{7.1}$$

where b_0, b_1 are related to λ_1, λ_2 via Eqs. (2.3), and to the scattering lengths through Eqs. (1.2). The values of b_0, b_1 from Eqs. (1.2) give the on-shell value of the parameters at pion threshold and these are the values used in (7.1) up to the Pauli corrected second order s-wave rescattering piece, (A10), which is normally added to b_0. However, b_0 or, equivalently, λ_1 is changed appreciably when one goes off shell. In infinite nuclear matter, where there is only forward propagation (conservation of a pion four-momentum in the interaction with infinite matter), the values needed for b_0 or λ_1 are only those at $t=0$ and hence the on-shell values. This is the formal justification for using the on-shell value for the parameters b_0, b_1 in Eq. (7.1), since this last equation implicitly assumes that the finite nuclei potential can be induced from the infinite matter results after implementing the local density prescription. However, in a finite nucleus, if the optical potential is used as an input to calculate the π nucleus T matrix, the pions in the optical potential in intermediate steps can be off the mass shell. Indeed, although the energy will be conserved because it is a good quantum number of the nucleon states in the nucleus, the momentum is certainly not, and thus momentum is not conserved. This is depicted in Fig. 18, where the value of $\mathbf{q}''$ can be, in principle, any one, thus leading to a momentum transfer even at threshold ($\omega=\mu$, $|\mathbf{q}| = |\mathbf{q}'| = 0$).

Since we saw that the t dependence in λ_1 of Eq. (5.1) was so important, we tend to think that this will have important repercussions in the lowest order optical potential. The immediate way to take this into account is to work with momentum space and use a potential of the type

$$\lambda_1(t)\tilde{\rho}(t) , \tag{7.2}$$

with

$$t = (\omega-\omega)^2 - (\mathbf{q}-\mathbf{q}')^2 = -(\mathbf{q}-\mathbf{q}')^2$$

instead of $\lambda_1\tilde{\rho}(t)$, where $\tilde{\rho}(t)$ is the Fourier transform of the nuclear density. Since in coordinate space Eq. (7.2) would give rise to a convolution of the nuclear density with the Fourier transform of $\lambda_1(t)$, we can thus interpret Eq. (7.2) as a way of considering the finite range of the interaction. In the case of a constant density ρ, we obtain from Eq. (7.2) the local density result $\lambda_1(t=0)\rho$. In a finite nucleus Eq. (7.2) will take account of changes of $\rho(\mathbf{r})$ at the nuclear surface. These ideas have been considered in Ref. 34.

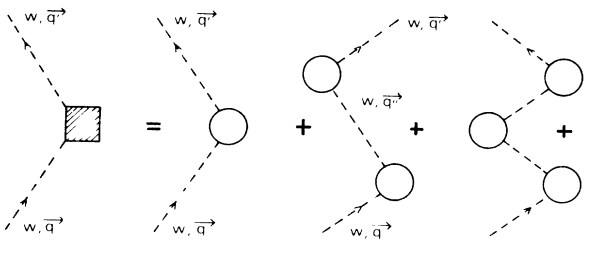

FIG. 18. Diagrammatic expression of the pion-nucleon t matrix constructed from the pion-nucleon optical potential. Square box: t matrix. Open circle: Optical potential.

In addition, one is adding the Pauli piece of Eq. (A10) in the lowest order. Note that Δb_0 of Eq. (A10) is not appreciably renormalized by these off-shell effects because most of the contribution in Δb_0 comes from b_1^2, and the b_1, or the λ_2, parameter is not so drastically changed by the off-shell extrapolation as b_0, or λ_1.

Intuitively, one might think that because the effect of the off-shell extrapolation is to increase effectively the b_0 value, one might get a repulsive effect in the potential which would have to be compensated for by an increase in the attraction of the second order optical potential (leading to positive values for the $\mathrm{Re}B_0$ parameter). The results are, however, surprising.[34] Instead of a repulsive effect, one actually finds an attractive effect and, in order to compensate, one needs a value of $\mathrm{Re}B_0^{\rm fit}$ even more negative than that quoted in Eq. (6.11), and therefore in stronger contradiction to our ultimate results written in Eq. (6.10). The attractive character of this interaction, also noticed in Ref. 14, has to be attributed to the nonperturbative character of the problem. The attraction comes ultimately after very subtle cancellations between the contribution to the energy shifts from small values of r, which is repulsive, and from large values of r, which is attractive. The cancellation is so much more subtle that it changes sign for pions of a few MeV of kinetic energy. This is found in Ref. 14, and agrees with the repulsive effects from this off-shell extrapolation found in Ref. 35 for low energy pion nucleus scattering.

The results of Ref. 34 should only be taken as indicative that the off-shell extrapolation of b_0 has important repercussions in the construction of the lowest order optical potential. The fact that a small change in energy changes the sign of the effect indicates that binding energies of the nucleons should also be considered and might have very important effects. Therefore an off-shell extrapolation not only on the momentum variables, as done up to here, but also on the energy variable, would have to be done.

A natural conclusion of the above discussion is that a proper way to deal with this problem would be to construct directly a potential, or even the T matrix without the need of the optical potential as the intermediate step,[49] by means of a microscopic scheme, working in momentum space and considering the contribution of each nucleon for the different nuclei. This procedure would, however, be extremely cumbersome in order to deal with the second order optical potential and also unnecessary. Indeed, we have already noticed that in the second order parameters most of the contribution comes from the parameter λ_2, which has a very smooth off-shell extrapolation compared with λ_1. In addition, we have already included these off-shell effects in the intermediate pions in our diagrams. Extending the range of q of these pions—because of the range allowed to the momenta of the external pions—would not alter appreci-

ably our results. This means that the treatment that we have given to these pieces along the lines in this paper is quite adequate and, indeed, is the most economical in view of the large number of considerations that its evaluation involved.

We could then conclude from this section that our study provides a reliable second order optical potential, within the uncertainties quoted, but that a proper treatment of the lowest order optical potential for the isoscalar part requires a delicate study beyond the scope of the present work.

VIII. CONCLUSIONS

We have presented here a new formalism to evaluate the s-wave optical potential for pionic atoms. Particular emphasis was put on calculating the second order piece in the density of this optical potential, which contains an absorptive (imaginary) and dispersive (real) part accounted for by the term $B_0\rho^2$, with B_0 a complex parameter.

Special care was taken in carrying out all the integrations without approximations. It was shown that this has important consequences in the evaluation of $\mathrm{Re}B_0$ and provides quite different results to other approaches that use dispersion relations and $\mathrm{Im}B_0$ from the absorption cut as an input. We have shown that such an approach should also consider the imaginary part of B_0 from the quasielastic cut and avoid typical approximations done in evaluating $\mathrm{Im}B_0$ from absorption. Failure to do both leads to highly unreliable results for $\mathrm{Re}B_0$.

We have also shown that the real part of B_0 coming from pion absorption into two particles and two holes is very small and most of the contribution to $\mathrm{Re}B_0$ comes from the excitation of the 1ph-1Δh component.

The effect of the Pauli blocking was shown to be moderate in $\mathrm{Im}B_0$, which justifies to some extent calculations done in the low density limit. However, the effects on the real part of B_0 were very important and led to reductions of 30%.

Another aspect that was considered was the effect of higher order corrections which were included in the parameter B_0. The renormalization of the pion propagators in the medium led to some enhancement with an increase of about 25% in $\mathrm{Im}B_0$. The values obtained for $\mathrm{Im}B_0$ are in agreement with present empirical values. The meson-nucleon form factors as well as nuclear short-range correlations were also considered and the results were quite stable under changes of these form factors or details of the correlations.

The off-shell effects, particularly those of the isoscalar part of the amplitude, had some repercussions on the problem and led to some increase in both the real and imaginary parts of B_0. On the other hand, when considering the off-shell effects in the isoscalar lowest order optical potential we noted that the effect was indeed important, but the results depended on subtle cancellations which suggested other methods than those used here in order to evaluate reliably this piece of the optical potential.

The implementation of the off-shell effects in the second order optical potential was much more straightforward, and much of the contribution came from the isovector λ_2 parameter, which is not so drastically affected by the off-shell extrapolation. This makes our evaluation of this part of the potential rather reliable. The imaginary part appears only in the second order optical potential and our results are in good agreement with experiment. The real part of the second order optical potential is attractive in our calculation and, together with the lowest order part of the optical potential, based on the LDA, and the Pauli rescattering term does not suffice to explain the empirically needed repulsion in the isoscalar s-wave part of the potential. The solution most probably lies in a proper treatment of the lowest order optical potential, incorporating off-shell effects in momentum and energy. However, a fully consistent treatment of these pieces would require a different formalism than the one used in this paper, and it still awaits an answer.

ACKNOWLEDGMENTS

While doing this work we benefited from discussions with R. Brockmann, W. Gibbs, K. Masutani, R. Seki, R. Silbar, and H. Toki. This work was supported in part by funds provided by the U.S. Department of Energy (DOE) under Contract No. DE-AC02-76ER03069 and by Comisión Asesora de Investigación Cientı. y Técnica.

APPENDIX A

We came to the pieces of the optical potential of Figs. 2–4 by considering the basic absorption diagram in Fig. 1. Now we would like to follow a different formal approach, more in connection with the developments of Ref. 3.

We will start with a $\pi\mathrm{N}\to\pi\mathrm{N}$ potential as input for the interaction Hamiltonian with matrix elements given by (we follow Bjorken-Drell[56] normalization of the fields)

$$\delta\tilde{H}=v(p',k';p,k)\ , \tag{A1}$$

with the same normalization as in (2.4b). In this way the standard scattering amplitude in the Born approximation is

$$f(p_i\to p_f)=-\frac{m}{4\pi\sqrt{s}}\delta\tilde{H}_{fi}\bigg|_{\text{on shell}}\ . \tag{A2}$$

Let us remark that the Hamiltonian in Eq. (A1) is the *elementary* interaction, while that in Eq. (2.4b) is an *effective* interaction, i.e., the t matrix obtained by iterating the elementary interaction, as will be shown below.

With the interaction Hamiltonian of (A1) we now construct all the many-body diagrams that contribute to the pion self-energy. These include all irreducible diagrams with two external pion legs and no external fermion legs. Here irreducible means that one cannot get two valid diagrams by cutting an internal pion line.[39,40] In this way one generates the sort of diagrams shown in Fig. 19. The analytical expression for these terms is then given by

$$-i\Pi(p)=\sum_{\substack{\text{spin}\\\text{isospin}}}\int\frac{d\mathbf{k}}{(2\pi)^3}n(\mathbf{k})\left[-iv(p,k;p,k)+\sum_{\substack{\text{spin}\\\text{isospin}\\\text{line } q}}\int\frac{d^4q}{(2\pi)^4}(-i)v(p,k;p+k-q,q)iD_0(p+k-q)iG_0(q)\right.$$

$$\left.\times(-i)v(p+k-q,q;p,k)+\cdots\right]. \tag{A3}$$

If D_0 and G_0 were the free pion and nucleon propagators the series in the large parentheses of (A3) can be immediately identified as the t matrix from the potential v:

$$t(p,k;p,k)=v(p,k;p,k)+i\sum_{\substack{\text{spin}\\\text{isospin}\\\text{line } q}}\int\frac{d^4q}{(2\pi)^4}v(p,k;p+k-q,q)D_0(p+k-q)G_0(q)t(p+k-q,q;p,k)\,, \tag{A4}$$

which can be expressed in a simpler way after the q^0 integration:

$$t(p,k;p,k)=v(p,k;p,k)+\sum_{\substack{\text{spin}\\\text{isospin}\\\text{line } q}}\int\frac{d\mathbf{q}}{(2\pi)^3}v(p,k;p+k-q,q)$$

$$\times\frac{1}{2\omega(\mathbf{p}+\mathbf{k}-\mathbf{q})}\frac{1}{p^0+k^0-\omega(\mathbf{p}+\mathbf{k}-\mathbf{q})-\varepsilon(\mathbf{q})+i\eta}t(p+k-q,q;p,k)\,. \tag{A5}$$

Hence the series of terms in (A3) can be summed up and we can express it as

$$-i\Pi^0(p)=\sum_{\substack{\text{spin}\\\text{isospin}}}\int\frac{d\mathbf{k}}{(2\pi)^3}n(\mathbf{k})(-i)t(p,k;p,k)\,, \tag{A6}$$

which gives the first term of the low density expansion for the optical potential.[3,57,58] We can express graphically the Lipmann-Schwinger equation of (A5) in Fig. 20, where the line f means free propagator. The diagram to the right of the equal sign signifies the free t matrix of Eq. (A5). Equation (A3) can now be expressed graphically if we allow only for free pion or nucleon propagators as shown in Fig. 21, where the line h stands for a hole line, implying a sum over occupied states. One can now easily go on and evaluate higher order terms in the density by modifying either the nucleon or the pion propagator in order to substitute the free propagator by the propagator in the medium. Let us first proceed with the modification to the nucleon propagator. We will take the same series of (A3) and take all terms where in one nucleon propagator we have substituted the propagator by the Pauli part of Eq. (2.8). This is depicted in Fig. 22, which also shows the obvious result of the summation. The piece after the equal sign in Fig. 22 is the well-known Pauli corrected second order rescattering piece for the s wave that has been formulated before in different languages.[1,3,20,24]

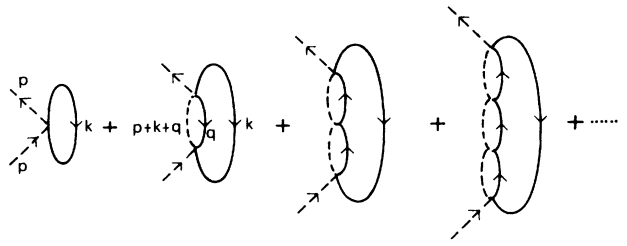

FIG. 19. Diagrams for the pion self-energy constructed from the πN potential of Eq. (A1).

The interesting feature of the approach which we are following is that the different pieces of the pion self-energy can be expressed in terms of the free πN scattering matrix (A5).[3]

Next, we would like to take medium modifications to the pion propagator. For this purpose we will follow the standard renormalization of the pion propagator by allowing an iterated series of ph or Δh excitations.[36] If we

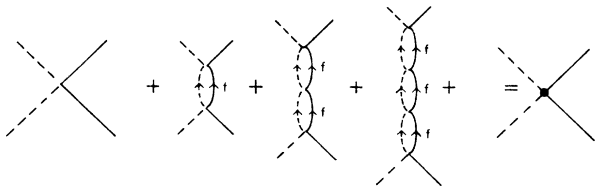

FIG. 20. Diagrams for the free πN t matrix constructed from the potential of Eq. (A1).

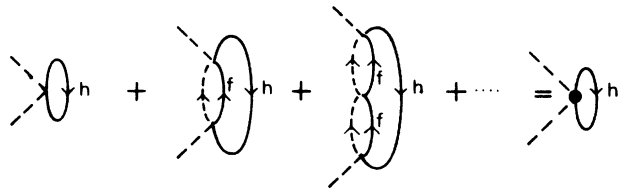

FIG. 21. Lowest order in density contribution to the pion self-energy.

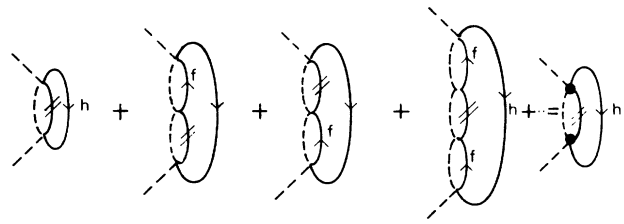

FIG. 22. Higher order corrections to the pion self-energy coming from the Pauli corrections to the nucleon propagator. The two short dashes stand for the Pauli correction to the nucleon propagator δG_P of Eq. (2.8). This piece is the second order Pauli corrected rescattering piece.

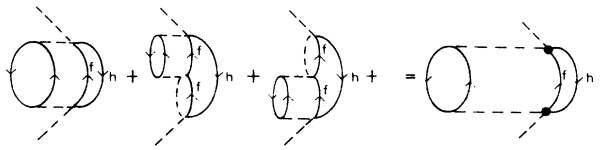

FIG. 23. Higher order corrections to the pion self-energy coming from the medium corrections to the intermediate pion propagators.

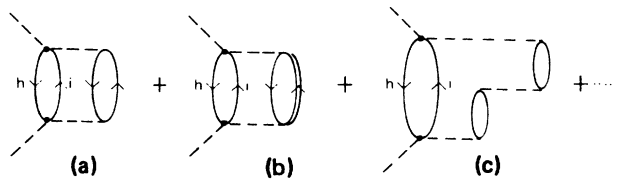

FIG. 24. same as Fig. 23, where the intermediate pion is allowed to be renormalized in the medium through a random-phase-approximation sum of ph and Δh excitations.

make such modifications to one of the pion propagators, we obtain the series of Fig. 23 with the obvious result shown there (we allow only one ph excitation for illustration purposes; the whole result is shown in Fig. 24). We can go one step further and substitute the free nucleon propagator in the diagram to the right of the equal sign in Fig. 23 by the medium propagator of Eq. (2.8). In this way it will now be a standard many-body diagram with the nucleon lines containing a particle and a hole line. Of course, only the particle line will contribute in this diagram. However, we can think in terms of the line f containing now the free and the Pauli piece of the propagator. If we take this last part, the diagram will be equivalent to that in Fig. 22 when we polarize the pion with a ph excitation. Thus one should not polarize the pion in Fig. 22 in order to avoid double counting if the diagram of Fig. 23 is considered in the standard many-body sense, which implies using for the propagator of the line f the medium propagator given by Eq. (2.8). One can, of course, repeat the procedure for the polarization of the pion through Δh and include the iteration of these pieces. This leads to the series of diagrams in Fig. 24, which correspond formally to those implicit in Fig. 4. In Refs. 20 and 21 the pion is polarized in the second order Pauli corrected rescattering piece of Fig. 22 (only through Δh excitation). If one wishes to do so, one must then add the diagrams on Fig. 24, though with line i as a free line. On the other hand, if one evaluates the series of diagrams of Fig. 24 in the standard many-body sense [keeping the nucleon medium propagator of Eq. (2.8) for the nucleon lines], then one should not include the polarization of the pion in the diagram of Fig. 24, but use only the free pion propagator in order to avoid double counting. We follow the latter procedure in the present work.

The different pieces of the optical potential that we have calculated rely on the free πN scattering matrix. In the energy and momentum range we consider in the present work, the amplitude is well reproduced by an s-wave part and a p-wave part. Since we are concerned with the s-wave optical potential, only the s-wave part of the amplitude has to be taken in the t matrix of the diagrams in Figs. 22–24. The diagram in Fig. 21 accounts for the lowest order optical potential in (1.1), the terms proportional to b_0, b_1. The terms in Fig. 24 are completely equivalent to those of Figs. 2–4. Since we need the free s-wave t matrix in the solid circles of the diagrams, we can once again use the effective interaction Hamiltonian of Eq. (2.4b), since it is meant to give the s-wave t matrix in lowest order.

We have thus used a different formal approach that does not rely on the process of pion absorption as an input. We have, however, obtained the same series of diagrams that we had before. At the same time we have obtained the lowest order optical potential and, in the same context, have obtained the s-wave Pauli corrected rescattering piece as well.

We are now ready to evaluate this latter piece, corresponding to the diagram of Fig. 22. By carrying out the energy integrations, the spin-isospin sums, and omitting the trivial isospin dependence, we get

$$\Pi^{\rm res}(p)=4\int\frac{d\mathbf{k}}{(2\pi)^3}\int\frac{d\mathbf{q}}{(2\pi)^3}n(\mathbf{k})n(\mathbf{q})\frac{1}{-p^0+\varepsilon(\mathbf{q})+\omega(\mathbf{p}+\mathbf{k}-\mathbf{q})-\varepsilon(\mathbf{k})+i\eta}$$
$$\times\frac{1}{2\omega(\mathbf{p}+\mathbf{k}-\mathbf{q})}(4\pi)^2\left[\left[\frac{2\lambda_1}{\mu}\right]^2+2\left[\frac{\lambda_2}{\mu^2}\right]^2[p^0+\omega(\mathbf{p}+\mathbf{k}-\mathbf{q})]^2\right]. \quad \text{(A7)}$$

In the low density limit and for $m\gg\mu$, this integral can be evaluated analytically and gives

$$\Pi(p^0=\mu,\ \mathbf{p}=\mathbf{0})=24\rho\frac{k_F}{\mu^2}(\lambda_1^2+2\lambda_2^2)\ , \quad \text{(A8)}$$

which by means of the relationship

$$\Pi(p)=-4\pi(1+\epsilon)b_0\rho \quad \text{(A9)}$$

can be effectively included in the lowest order term of the optical potential by incorporating a correction to the parameter b_0,

$$\Delta b_0=-\frac{6k_F}{\pi\mu^2}\frac{1}{1+\epsilon}(\lambda_1^2+2\lambda_2^2)\ , \quad \text{(A10)}$$

in agreement with Refs. 1, 20, 21, and 34.

APPENDIX B

We would like to compare the extrapolation of Eq. (5.1) with others existing in the literature. In Refs. 59–62 the authors use field theoretical methods and constraints from current algebra to extract the amplitude off-shell. Reference 63 uses the same current algebra constraints and works out useful interpolations between known points. Reference 64 assumes separable potentials and determines the off-shell extrapolation by means of dispersion relations.

We have followed the different approaches and evaluated the isoscalar part of the s-wave amplitude, the most sensitive to the off-shell extrapolation, for the situation found in pionic atoms. For not too large values of the kinematical variables, the isoscalar amplitude satisfying the current algebra constraints can be written as[63]

$$\bar{F}^+(\nu,t;q^2,q'^2)=\left[\frac{t}{\mu^2}-1\right]\frac{\sigma(t)}{f_\pi^2}$$
$$+(q'^2+q^2-t)\frac{\bar{F}^+(0,\mu^2;\mu^2,\mu^2)}{\mu^2}$$
$$+f_3^+\nu^2\ , \quad \text{(B1)}$$

where the first term on the right-hand side is the Adler term and $\sigma(t)$ is the πN sigma commutator.[61] The variable t is the four-momentum transfer, $t=(q-q')^2$, and $\nu=(q+q')\cdot(p+p')/4m$, where q,q' are the initial and final pion tetramomenta and p,p' the same variables for the nucleons. By following Ref. 60, we take, for $\sigma(t)$,

$$\sigma(t)=\frac{\sigma(0)}{(1-t/\mu_1^2)^2(1-t/\mu_2^2)}\ , \quad \text{(B2)}$$

with $\mu_1=8.24\mu$, $\mu_2=7.5\mu$, and $\sigma(0)=25$ MeV (Refs. 59 and 60). For the other variables we take $f_\pi=93$ MeV, $f_3^+=0.82\mu^{-1}$, and $F^+(0,\mu^2;\mu^2,\mu^2)=-0.30\mu^{-1}$, the latter in the range of accepted values[60] such that Eq. (B1) gives the appropriate on-shell value at threshold through the relationship

$$\bar{F}^+(\nu,t;q^2,q'^2)\,|_{\text{on shell}}=-\frac{4\pi 2\lambda_1}{\mu}\ . \quad \text{(B3)}$$

The amplitude of Ref. 64 for the half-shell situation that one finds in the diagram of Fig. 2 can also be evaluated easily. This provides a function $b_0(q')$ to replace the b_0 parameter given by

$$b_0(q')=\frac{1}{3}\left[\frac{v_1(q')}{v_1(0)}a_1+2\frac{v_3(q')}{v_3(0)}a_3\right]\ , \quad \text{(B4)}$$

where the vertex functions $v_1(q'),v_3(q')$ are evaluated in Ref. 64. The results of these different extrapolations are shown in Fig. 14.

*Permanent address: Instituto de Física Corpuscular, Centro Mixto Universidad–Consejo Superior de Investigaciones Científicas, Facultad de Ciencias Físicas, Universidad de Valencia, Burjasot (Valencia), Spain.

[1]M. Ericson and T. E. O. Ericson, Ann. Phys. (N.Y.) **36**, 323 (1966).
[2]G. Höhler, F. Kaiser, R. Koch, and E. Pietarinen, Handbook of Pion-Nucleon Scattering [Physics Data **12-1** (1979)].
[3]J. Hüfner, Phys. Rep. **21**, 1 (1975).
[4]E. Oset and L. L. Salcedo, Nucl. Phys. **A468**, 631 (1987).
[5]E. Oset, Y. Futami, and H. Toki, Nucl. Phys. **A448**, 597 (1986).
[6]M. Krell and T. E. O. Ericson, Nucl. Phys. **B11**, 521 (1969).
[7]L. Tauscher and W. Schneider, Z. Phys. **271**, 409 (1974).
[8]C. J. Batty *et al.*, Nucl. Phys. **A322**, 445 (1979).
[9]E. Friedman and A. Gal, Nucl. Phys. **A345**, 457 (1980).
[10]R. Seki, M. Oka, K. Masutani, and K. Yazaki, Phys. Lett. **97B**, 200 (1980).
[11]K. Stricker, J. Carr, and H. McManus, Phys. Rev. C **22**, 2043 (1980).
[12]E. Friedman, Phys. Lett. **104B**, 357 (1981).
[13]T. E. O. Ericson and L. Tauscher, Phys. Lett. **112B**, 425

(1982).
[14]R. Seki and K. Masutani, Phys. Rev. C **27**, 2799 (1983); R. Seki, K. Masutani, and K. Yazaki, *ibid.* **27**, 2817 (1983).
[15]C. J. Batty *et al.*, Phys. Rev. Lett. **40**, 931 (1978).
[16]C. J. Batty *et al.*, Nucl. Phys. **A322**, 445 (1979).
[17]R. J. Powers *et al.*, Nucl. Phys. **A336**, 475 (1980).
[18]L. Tauscher, C. García-Recio, and E. Oset, Nucl. Phys. **A415**, 333 (1984).
[19]G. A. Miller and J. V. Noble, Phys. Rev. C **22**, 1211 (1980).
[20]H. McManus and D. O. Riska, J. Phys. G **7**, L153 (1981).
[21]D. O. Riska, Nucl. Phys. **A377**, 319 (1982).
[22]K. Brueckner, Phys. Rev. **98**, 769 (1955).
[23]D. Beder, Nucl. Phys. **B14**, 586 (1969).
[24]K. Nishimoto, H. Ohtsubo, and H. Narumi, Prog. Theor. Phys. **46**, 135 (1971).
[25]C. B. Dover, J. C. Ballot, and R. H. Lemmer, Lett. Nuovo Cimento **2**, 715 (1971).
[26]C. B. Dover, Ann. Phys. (N.Y.) **79**, 441 (1973).
[27]G. F. Bertsch and D. O. Riska, Phys. Rev. C **18**, 317 (1978).
[28]F. Hachenberg and H. J. Pirner, Ann. Phys. (N.Y.) **112**, 401 (1978).
[29]J. Chai and D. O. Riska, Phys. Rev. C **19**, 1425 (1979).
[30]G. A. Miller and J. V. Noble, Phys. Rev. C **21**, 2519 (1980).
[31]M. Brack, D. O. Riska, and W. Weise, Nucl. Phys. **A287**, 425 (1977).
[32]O. V. Maxwell, W. Weise, and M. Brack, Nucl. Phys. **A348**, 388 (1980); O. V. Maxwell and W. Weise, *ibid.* **A348**, 429 (1980).
[33]O. Scholten *et al.*, Phys. Rev. C **32**, 653 (1985).
[34]C. García-Recio, R. Brockman, E. Oset, and H. Toki, An. Fís. **83**, 127 (1987).
[35]R. S. Bhalerao and C. M. Shakin, Phys. Rev. C **23**, 2198 (1981).
[36]G. E. Brown and W. Weise, Phys. Rep. **22**, 279 (1975).
[37]E. Oset, H. Toki, and W. Weise, Phys. Rep. **83**, 281 (1982).
[38]D. S. Koltun and A. Reitan, Phys. Rev. **141**, 1413 (1966).
[39]E. Oset, in *Proceedings of the Vth Topical School on Quarks, Mesons and Isobars in Nuclei,* Granada, 1982, edited by R. Guardiola and A. Polls (World-Scientific, Singapore, 1983), p. 1.
[40]A. L. Fetter and J. D. Walecka, *Quantum Theory of Many-Particle Systems* (McGraw-Hill, New York, 1971).
[41]E. Oset and A. Palanques, Nucl. Phys. **A359**, 289 (1981).
[42]P. A. Dominguez and B. J. Verwest, Phys. Lett. **89B**, 333 (1980).
[43]J. W. Durso, A. D. Jackson, and B. J. Verwest, Nucl. Phys. **A282**, 404 (1977).
[44]C. A. Dominguez, Phys. Rev. C **24**, 2611 (1981).
[45]R. Machleidt, in *Quarks, Mesons and Isobars in Nuclei,* edited by R. Guardiola and A. Polls (World-Scientific, Singapore, 1983), p. 278; K. Holinde, Phys. Rep. **68**, 121 (1981).
[46]C. García-Recio, Ph.D. thesis, University of Valladolid, 1986.
[47]G. Hamilton, in *High Energy Physics,* edited by E. H. S. Burhop (Academic, New York, 1967), Vol. I, p. 194.
[48]W. Weise, Nucl. Phys. **A278**, 402 (1977).
[49]E. Oset and W. Weise, Nucl. Phys. **A319**, 477 (1979).
[50]A Hosaka, K. I. Kubo, and H. Toki, Nucl. Phys. **A444**, 76 (1985), and private communication.
[51]D. O. Riska and H. Sarafian, Phys. Lett. **95B**, 185 (1980).
[52]G. E. Brown, *Many-Body Problems* (North-Holland, Amsterdam, 1972).
[53]V. R. Pandharipande and R. B. Wiringa, Rev. Mod. Phys. **51**, 821 (1979).
[54]A. D. Jackson, A. Landé, and R. A. Smith, Phys. Rep. **86**, 55 (1982).
[55]R. Brockmann and E. Oset, Phys. Lett. **118B**, 33 (1982).
[56]J. D. Bjorken and S. D. Drell, *Relativistic Quantum Fields* (McGraw-Hill, New York, 1965).
[57]C. B. Dover, J. Hüfner, and R. H. Lemmer, Ann. Phys. (N.Y.) **66**, 248 (1971).
[58]J. Hüfner and C. Mahaux, Ann. Phys. (N.Y.) **73**, 525 (1972).
[59]W. T. Huang, C. A. Levinson, and M. K. Banerjee, Phys. Rev. C **5**, 651 (1972).
[60]M. K. Banerjee and J. B. Cammarata, Phys. Rev. D **16**, 1334 (1977); C **17**, 1125 (1978); D **18**, 4078 (1978).
[61]M. K. Banerjee, in *Meson-Nuclear Physics—1979 (Houston),* Proceedings of the 2nd International Topical Conference on Meson-Nuclear Physics, AIP Conf. Proc. No. 54, edited by E. V. Hungerford III (AIP, New York, 1979), p. 30.
[62]M. J. Reiner, Ann. Phys. (N.Y.) **154**, 24 (1984).
[63]S. A. Coon *et al.*, Nucl. Phys. **A317**, 242 (1979).
[64]G. T. Londergan, K. W. McVoy, and E. J. Moniz, Ann. Phys. (N.Y.) **86**, 147 (1974).